OPTIMIZING THE EFFICIENCY OF CYLINDRICAL CYCLONE GAS/LIQUID SEPARATORS FOR FIELD APPLICATIONS

A Thesis

by

ADEDEJI ADEBARE

Submitted to the Office of Graduate Studies of
Texas A&M University
in partial fulfillment of the requirements for the degree of

MASTER OF SCIENCE

August 2006

Major Subject: Petroleum Engineering

OPTIMIZING THE EFFICIENCY OF CYLINDRICAL CYCLONE GAS/LIQUID SEPARATORS FOR FIELD APPLICATIONS

A Thesis

by

ADEDEJI ADEBARE

Submitted to the Office of Graduate Studies of
Texas A&M University
in partial fulfillment of the requirements for the degree of

MASTER OF SCIENCE

Approved by:

Chair of committee,	Stuart L. Scott
Committee Members,	Jerome Schubert
	Yassin Hassan
Head of Department,	Steve A. Holditch

August 2006

Major Subject: Petroleum Engineering

ABSTRACT

Optimizing the Efficiency of Cylindrical Cyclone Gas/Liquid Separators for Field Applications.

(August 2006)

Adedeji Adebare, B.S., Obafemi Awolowo University, Ile-Ife, Nigeria

Chair of Advisory Committee: Dr. Stuart L. Scott

Problems associated with the use of compact cylindrical cyclone gas/liquid (CCGL) separators can be attributed to two physical phenomena: gas carry-under and liquid carry-over (LCO). Inadequate understanding of the complex multiphase hydrodynamic flow pattern inside the cylindrical separator has inhibited complete confidence in its design and use, hence the need for more research.

While many works have been done with a fixed inlet slot to predict the operational efficiency of the cyclone separator, very little is known about how separator performance can be influenced due to changes in fluid properties. During the operations of the CCGL separator the complex flow situations arising from severe foaming within the separator has not been addressed. Also the effects of emulsion formation under three phase flow conditions on the properties of cyclone separators are yet to be studied.

An understanding of liquid holdup and hydrodynamic nature of flow in a compact separator under zero net liquid flow (ZNLF) and zero net gas flow (ZNGF) conditions is necessary in many field applications, especially for the prediction of LCO and in the design of the CCGL separators. Also, ZNLF holdup is an important parameter in predicting bottom-hole pressures in pumping oil wells.

This research investigated the effects of fluid properties such as density, foam and emulsion formation on ZNLF, zero net gas flow ZNGF, and LCO in compact cyclone separators; this was achieved by replacing water, which is the conventional fluid used as the liquid medium in many previous research efforts with a foamy oil while maintaining air as the gas phase. Variable-inlet-slots that regulate the artificial gravity environment created by the separator were used to check for improved separator performance. Also

experiments to check separator response to a range of water-cut in three-phase flow were performed. All experiments were carried out under low constant separator pressures.

The ZNLF holdup is observed to decrease as the density of the fluid medium decreases. Varying the inlet slot configurations and recombination points does not have any effect on the ZNLF holdup when changes in density of the liquid phase occur. Comparisons with previous work show that there exists a wide variation in the LCO operational envelope when severe foaming occurs in the CCGL separator. At high water-cut (greater than 30%), the separator LCO performance was observed to be normal. However, at water-cut below 30%, LCO was initiated much earlier; this is attributed to severe foaming in the CCGL separator.

DEDICATION

I dedicate this research effort to the almighty God, my parents — Mr. & Mrs. Adebare, my siblings, members of petroleum engineering faculty at Texas A&M University, and my colleagues.

ACKNOWLEDGMENTS

I wish to express my gratitude to my advisor Dr. Stuart Scott for his numerous inputs and suggestions to my academic progress, his moral support and understanding during my stay in A&M are highly appreciated.

My appreciation also goes to all the members of my research committee, Dr. Jerome Schubert, and Dr. Yassin Hassan, for their constructive criticisms of this project.

I will like to recognize the financial contributions of Multiphase Research Group and sponsors at Texas A&M University towards the successful completion of this research.

And to all friends and colleagues at TAMU and beyond, I say thank you all for being there for me when it mattered most and may God bless you all.

TABLE OF CONTENTS

CHAPTER Page

LIST OF FIGURES

Page

Page

LIST OF TABLES

Page

CHAPTER I

INTRODUCTION

1.1 Background

The multiphase separation technology currently in place in the oil and gas industry is primarily based the use of vessel-type separator which is large, heavy, and expensive to purchase, operate, and maintain. No significant improvements on this technology have been reported over the last couple of years. Recently, there are moves within the industry to develop alternative technologies to the vessel-type separator. One such alternative is the use of compact or in-line separators, such as CCGL separator. The CCGL is an emerging class of vertical compact separators, as compared to the very mature technology of the vessel-type separator.

A separator is a field vessel used to separate gas, oil, and water from a multiphase mixture produced from oil and gas wells. Unlike bulky vessel-type separators, the CCGL separator is a simple, compact, low-cost, low-weight separator and is easy to install and operate. CCGL separator technology is a relatively new technology in multiphase flow separation processes since it is basically a vertical piece of pipe, with a downward-inclined tangential inlet and two outlets, one at the bottom and the other at the top, it is also low maintenance. Therefore, it is gaining popularity as an economically attractive alternative for the conventional separation tank in many operating environments such as offshore and arctic operations where space and weight are at a premium.

Current applications of the cylindrical cyclone are for separating gas and liquid. The two-phase mixture flows tangentially from the inlet into the cylindrical cyclone in a swirling motion, forming a vortex. Centrifugal force moves the gas to the center, upward, and out from the top of the column, while gravitational and buoyancy forces move the liquid radially toward the wall, downward, and out from the lower part of the column.

This thesis follows the style and format of the *Journal of Petroleum Technology*.

The cylindrical cyclone separator has a wide range of potential applications, varying from only partial separation to complete phase separation. Potential applications include control of the gas/liquid ratio for multiphase flow meters, pumps, and desanders, portable well-test metering, steam-quality metering, flare-gas scrubbing, primary surface and subsurface separation, and preseparation upstream of slug catchers or primary separators.

The operation of the CCGL is greatly affected by two known limiting physical phenomena: liquid carry-over (LCO) and gas carry-under (GCU). LCO is initiated in the form of droplets or stratified flow in the upper section while GCU could be observed as entrained gas bubbles with the discharged liquid stream at the lower part of the column. Inadequate understanding of the complex multiphase hydrodynamic flow pattern inside the cylindrical separator has inhibited complete confidence in its design and use.

In the past, research and design efforts to improve the performance of the CCGL have focused on areas such as inlet geometry, hydrodynamic flow behavior in the CCGL, liquid level controller etc. nothing has been reported on the effects of foam and emulsion formation on ZNLF, ZNGF, and LCO which are used for design considerations. Therefore, a good knowledge of CCGL response to multiphase flow conditions involving foam and/or emulsion formation will aid proper CCGL design and ultimately, confidence in its use.

1.2 Literature review

Previous studies on the CCGL separator have focused on mechanistic models capable of predicting the operational envelope for liquid carry-over and on understanding the flow field in the CCGL. Other works have investigated the behavior of small gas bubbles in the lower part of the CCGL, below the inlet and the related gas carry-under phenomena. Erdal *et al.* [1] and Motta *et al.*[2] confirmed that a complex swirling flow occurs in the CCGL. These studies used flow visualization experiments and computational fluid dynamics (CFD) simulations to investigate the effects of the gas phase on flow behavior below the inlet.

Arpandi *et al*.,[3] by Mohan *et al.*, [4] and Gomez *et al.*[5] have published detailed reviews on compact separation technology research. Shoham and Kouba[6] recently presented a summary of the state-of-the-art of cylindrical cyclone technology. From an experiment to investigate the effects of density and viscosity on ZNLF in vertical pipes, An *et al*.[7] found that that ZNLF holdup decreases as the superficial gas velocity increases.

Duncan and Scott[8], by the use a field-scale experiment, discovered that pressure has a significant impact on liquid holdup for vertical ZNLF. They indicated that the existing model of liquid holdup poorly predicts behavior for pressure greater than 100 psig. They proposed a methodology to improve both the stability of the existing model and its ability to predict high pressure liquid holdup behavior.

Reydon and Gauvin[9] showed that an increase in the magnitude of the inlet velocity does not change the shapes of the tangential velocity, axial velocity, and the static pressure profiles but increases their respective magnitudes. Millington and Thew.[10] reported Local laser Doppler anemometer (LDA) velocity measurements in cylindrical cyclone separators. They suggested the use of twin, diametrically opposite inlets for greater axisymmetry and gas core filament stability, leading to a much improved gas carry-under performance. They made the important observation that the vortex occurring in the cylindrical cyclone separator is a forced vortex with a tangential velocity structure.

Farchi's[11] measurements of tangential velocity in a cylindrical cyclone with static pitot tubes confirmed that a forced vortex occurs in the cyclone. However, as the diameter of the cyclone increases, the velocity distribution tends to match the free vortex profile. Through a study on gas/liquid flow characteristics in a spiral horizontal cyclone with vortex generator, Kurokawa and Ohtaik[12] confirmed the existence of a complex velocity profile by accurate single-phase liquid flow measurements. The study distinguishes a forced vortex generating a jet region with extremely high swirl velocity around the pipe center from a second swirl region formed by a free vortex near the wall and also an intermediate region of backflow with high swirl velocity.

Barbuceanu and Scott[13] found that the performance of the CCGL can be improved more than three times using a new design of inlet geometry. The actual area of possible operational envelope expansion of a cylindrical cyclone gas/liquid separator, by means of a variable inlet-slot configuration, is in the gas carry-under performance. Igho[14] found

that the inlet-slot size variation has no noticeable effect or improvement on the liquid carry-over performance of the separator; agreement between the theoretical analysis and experimental verification of the expanded GCU operational envelope achievable by the use of variable-inlet slots in a CCGL separator is good.

Few mechanistic models have been developed recently to describe and predict the flow behavior in the cylindrical cyclone. A mechanistic model for predicting separation efficiency based on the analysis of droplet trajectories in liquid/liquid, oil/water hydro-cyclones was presented by Wolbert *et al.*[15] These trajectories were calculated through a differential equation combining models for the three bulk velocity distributions, namely, axial, radial, and tangential.

Arpandi *et al.*[3] developed a mechanistic model capable of predicting the general hydrodynamic flow behavior in a cylindrical cyclone separator from experimental and theoretical studies performed in the Tulsa U. Separation Technology Projects (TUSTP).This includes simple velocity distributions, gas/liquid interface shape, equilibrium liquid level, total pressure drop, and operational envelope. An analysis of bubble trajectory for cylindrical cyclone separators was presented by Marti *et al.*[16] The model predicts the gas/liquid interface vortex near the inlet as a function of the radial distribution of the tangential velocity. A bubble trajectory analysis enables the determination of separation efficiency based on the gas bubble size.

Movafaghian[17] presented new experimental data on the effects of geometry, fluid physical properties, and pressure on the hydrodynamic flow behavior in cylindrical cyclone separators to verify and refine the cylindrical cyclone mechanistic model developed previously by Arpandi *et al.*[3] Wang *et al.*[18] developed a steady-state and a dynamic model as the framework for cylindrical cyclone passive and active control, respectively. They used the steady-state model to analyze the system sensitivity and the dynamic model to analyze the system stability by applying linear control theory. In this investigation, they presented a preliminary control strategy for cylindrical cyclone control system design.

Mantilla *et al.*[19] presented a set of correlations for the prediction of the velocity field in the cylindrical cyclone tangential and axial directions. Their improved bubble trajectory model showed good agreement with the experimental data. Gomez *et al.*[20]

developed a state-of-the-art computer simulator for cylindrical cyclone design in an Excel Visual Basic platform that is capable of integrating the different modules of the mechanistic model. Model enhancements include a flow-pattern-dependent nozzle analysis for the .unified particle trajectory model for bubbles and droplets, including a tangential velocity decay formulation, and a simplified model for the prediction of the cylindrical cyclone aspect ratio.

1.3 Objectives of the research

The purpose of this research effort is to verify and quantify the effects of foam generation on zero net liquid flow (ZNLF), zero net gas flow (ZNGF), and liquid carry-over (LCO) properties of the CCGL separator. This involves replacing the liquid medium usually water with a highly foamy liquid such as mineral oil while maintaining air as the gas phase. The resulting operational envelope will be compared with previous works where water was used as the liquid phase Also, a similar experimental investigation with three-phase flow system involving air, water, and foamy oil in a range of water cut will be performed. This is aimed at checking separator performance when a mixture of oil and water acts as the single phase liquid in the multiphase feed into the CCGL.

1.4 Thesis outlook

The physical geometry and operations of the CCGL separator will be illustrated followed by a discussion on its current applications. The limiting physical phenomena associated with the separator performance will be described. A general overview of the experimental facility and process is given.

The effect of foam on the efficiency of the CCGL separator is presented for different separator properties like zero-net liquid flow situations, zero-net gas flow, and liquid carry-over. Analysis of the results obtained from this investigation compared with previous works is reported.

Finally, conclusions and recommendations deduced from the outcome of this research are outlined.

CHAPTER II

PHYSICAL GEOMETRY AND OPERATIONAL FEATURES OF CCGL SEPARATORS

2.1 Physical geometry of the gas/liquid cylindrical cyclone separator

The CCGL separator consists of transparent acrylic pipes. CCGL is a 3 inch. ID pipe mounted vertically with a combined height of 8 feet. The height is divided by the inlet into lower liquid leg and upper gas leg. The liquid and gas sections are made up of 3-inch PVC pipes. Absolute and differential pressure transducers are mounted all around the CCGL loop to measure pressure as seen in **Fig. 2.1**.

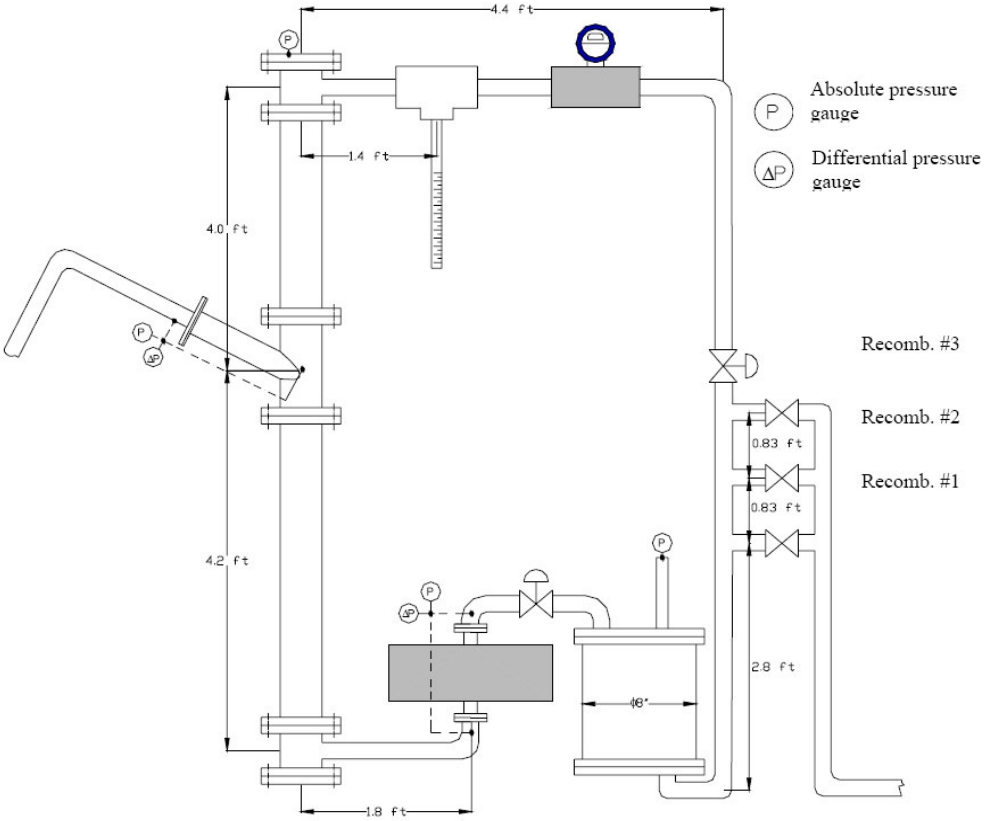

Fig. 2.1—Schematic of CCGL separator test loop (Igho[14]) will permit gas and liquid separation.

Two-phase flow is fed into the CCGL, about 4 feet below the exit of the gas section, through a 2-inch ID, 27 degree downward inclined tangential inlet. The outlet section is designed to recombine the gas and liquid legs as in metering applications or full separation of gas and liquid streams. Three different recombination points are available utilizing the three different valves at the exit of the CCGL loop, as could be seen in the figure.

2.2 Operations of CCGL separators

The CCGL operations is based on buoyancy, gravity and, centrifugal forces. A multiphase stream comprising of water, oil, and gas is fed into the separator, the ensuing mixture spins rapidly round the wall of the pipe, and the momentum of the process fluid combined with the tangential inlet generates a liquid vortex with sufficient G-forces for gas and liquid separation **Fig. 2.2**. Due to gravity and centrifugal forces, the liquid phase is separated from the multiphase mixture and exits through the lower section of column, while the gas moves through the vortex to exit at the upper section of the column due to buoyancy effects.

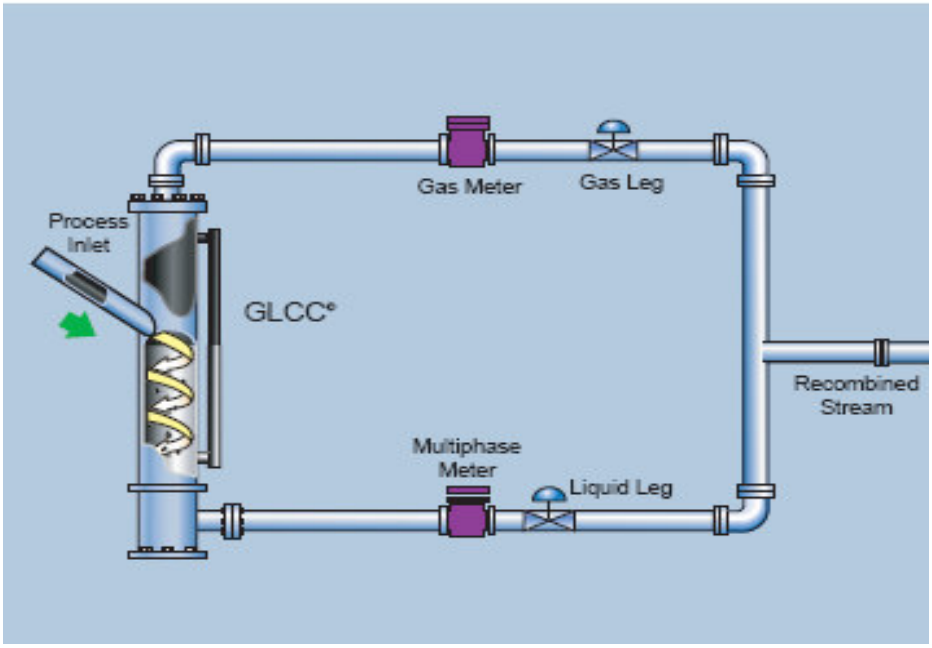

Fig. 2.2—CCGL separator operation involving gas and liquid separation

2.3 Performance and applications

The CCGL, primarily used for bulk separation, can be designed for various degrees of performance. Typical performance levels from the CCGL are 0.5–2.0 gallons of liquid per MMscf in the gas outlet and 0-5% gas volume fraction (GVF) in the liquid outlet.
Fluid flows with a liquid-to-gas ratio of greater than 50 barrels of liquid per MMscf of gas are the preferred feed for the CCGL. The CCGL can be applied successfully in a number of operations as listed below:

- Control of gas-liquid ratio for multiphase flow meters, pumps and desanders
- Portable well test metering
- Steam quality metering
- Inlet or wellhead test separators
- Flare gas scrubbing
- Two-phase production separators
- Flash separators before oil treaters or water treating equipment
- Vessel debottlenecking through the removal of excess gas from the flow stream in advance of the problem vessel
- Pre separation upstream of slug catcher
- Primary surface or sub-sea separation

The CCGL is frequently used for applications where only partial separation of gas from liquid is needed. An example of such application is the partial separation of gas from high pressure wells and the gas is used for gas lift of low pressure wells. The CCGL is a key element in the design for gas lift system. When the CCGL is in operation, it eliminates the need for gas compressors and pipelines to and from individual wells. Removing a significant portion of the gas will reduce fluctuations in the liquid flow and may result in improved performance and smaller units of other downstream separation devices. Total or partial gas/liquid separation can improve the accuracy of individual phase rate measurement in a multiphase metering loop system.

The CCGL when used as a multiphase metering loop system have many advantages over either conventional separation units with single-phase measurement or non-separating multiphase meters. Significant advantages of the CCGL over the conventional vessel tank separators are

- Simplicity in construction
- Ease of operation
- Compactness (smaller footprint and space)
- Low weight
- Low capital and operational cost
- Less inventory

Currently, there are over 700 CCGL separators in operation, both offshore and onshore oil fields applications. Approximately 80 CCGL multiphase metering loops have been installed in Oklahoma. These applications are mainly for oil flow rate of 1,500 bbls per day and a GOR (gas-oil ratio) of 500. In some cases, a single CCGL is used for multiple wells. In terms of cost comparison, CCGL unit costs about $7,500 compared to $25,000 for conventional separator. **Fig. 2.3** is a unit of CCGL separator installed for metering purposes during field operations.

Fig. 2.3—A unit of CCGL separator consisting of pipe sections and meters installed for field application involving gas and liquid separation (from Petroleum Technology Transfer Council, 2002)

2.4 Physical features and design criteria of CCGL separators

There are two main known physical phenomena that inhibits the operational efficiency of the compact cyclone separator, they are liquid carry-over (LCO) and gas carry-under (GCU). The extent to which these limiting phenomena can affect the separator performance are dictated by the shape and velocity of the multiphase feed into the separator body, complex hydrodynamics flow pattern within the separator, zero net-liquid flow, zero net-gas flow, the equilibrium liquid level (ELL), and the physical geometry of the CCGL separator. The following is a brief description of these properties.

2.4.1 Liquid carry-over (LCO)

Liquid carry-over is described as the initiation of liquid droplets in the exiting gas stream at the top of the cyclone separator. This phenomenon is formed when the separator is operating under extreme conditions of either high gas or liquid flow rates. The operational envelope for the LCO of the CCGL separator is obtained by plotting the superficial liquid velocity or liquid flow rate against superficial gas velocity or gas flow rate at which LCO is initiated as seen in **Fig. 2.4**.

In the figure, the thick line represents the operational envelope; the area under the envelope describes the region of efficient operation, no LCO for flow conditions within this region. While above the line represents region of perpetual LCO situations. The factors responsible for the shape and magnitude of the operational envelope as will be demonstrated later are operating pressure, equilibrium liquid level, fluid viscosity, foam and emulsion formation.

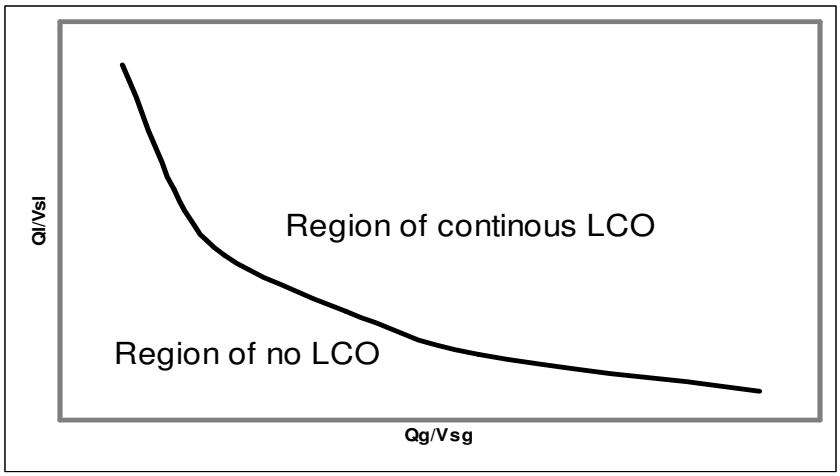

Fig. 2.4—Liquid carry-over operational envelope

2.4.2 Gas carry-under (GCU)

Gas carry-under is defined as the onset of gas bubbles in the discharged liquid stream from the bottom of the separator column. The tangential geometry of the separator entry and velocity of the fluid flowing into the separator creates a vortex at the lower part of the separator, gas bubbles move radial inward forming a gas-core-filament. The phenomenon of GCU is affected by several factors which included the length of the lower segment, the dimension of the separator inlet, flow pattern into the inlet section, and the magnitude of the force created for separation, this force is known as the g-force which is defined as the ratio of the tangential/centrifugal acceleration to the acceleration due to gravity.

Previous works have put g's for efficient CCGL performance to be in the range of 50 to 100. A number of mechanisms are responsible for GCU initiation, these are shallow radial trajectory of individual gas bubbles preventing coalescence with the gas core filament, and this is attributable to improper design of the lower section of the separator. Gas core filament instability, this occurs during helical whipping of the gas core filament leading to the filament breaking-off forming small bubble that are swept away by the exiting liquid stream (a case of poor inlet design). Bubble swarm instability occurring during abrupt increase in liquid rate producing a cluster of bubbles that slips away from the gas-core filament and escape with the exiting liquid stream.

2.4.3 Equilibrium liquid level (ELL)

Equilibrium liquid level can be described as a range of possible movement liquid level within the separator body and the operational envelope to maintain efficient separation. The ELL is determined by the pressure balance from the exit of the gas section and the liquid section and is obtain by the use of a liquid level indicator (sight gauge).

2.4.4 Zero-net gas flow (ZNGF)

Zero-net gas flow is the maximum liquid flow rate that the separator can tolerate prior to commencement of liquid carry-over phenomenon for a zero gas flow rate. The zero-net gas flow is significantly influenced by the property of the mixture such as foam and viscosity. Adequate design of the length of lower part of separator and lateral liquid outlet of separator in addition to special flow pattern conditions such as large tangential acceleration will mitigate this effect.

2.4.5 G-force for three-phase flow and design of the CCGL separators.

The design of the CCGL is affected by the velocity and nature of the stream flow as revealed by this research. CCGL separation performance is a function of the tangential velocity at the inlet. The mixture tangential velocities are important in predicting the flow behavior, describing the vortex interface, determining droplet paths, and in estimating the G-force required for efficient separation. The G-force is a parameter that is used to quantify the force applied on the fluid mixture leading to separation within the CCGL separators. The G-force is defined as the ratio of the tangential/centrifugal acceleration to the acceleration due to gravity.

The G-force can be obtained by the following relation

$$G - force = \frac{a_c}{g} \tag{2.1}$$

The centrifugal acceleration is expressed as

$$a_c = \frac{V_{tm}^2}{r}\cos\alpha \qquad (2.2)$$

And the mixture tangential velocity

$$V_{tm} = \frac{Q_{Lmix} + Q_G}{A_{in}} \qquad (2.3)$$

Where

$$Q_G = kM_R \qquad (2.4)$$

And

$$k = 0.307\frac{zT}{P_{in-situ}} \qquad (2.5)$$

2.5 Properties of fluid flow in CCGL separators

Most of the studies on gas/liquid cylindrical cyclone separator have been focused on the inlet geometry design, the use of liquid level controllers etc. Little or no effort has been made to determine the impact of foam generation and emulsion formation on the performance of the CCGL separators.

2.5.1 Foam

Foam could be described as the dispersion of gas in liquid, usually with a surface-active agent present. Foams are not thermo-dynamically stable and ultimately decay into their constituent phases, but can be mechanically stable. When foam exists inside a

confining medium, dimension of this confining medium relative to the average bubble size determine the texture and properties of the foam.

When the confining diameter is large relative to typical bubble size, such as in a pipe, the foam is similar to bulk foam. Its flow can then be treated as that of a non-Newtonian, compressible pseudofluid. Where the diameter of the confining body is comparable to, or smaller than the minimum bubble size, the foam exists as a network of lamellae rather than bubbles. Such lamellar-structure foam can not be treated as a single fluid, because liquid and gas flows by different mechanisms[21]. Holm[22] found liquid to flow as a continuous phase, but gas flow to occur by a sometimes very slow process of continually breaking and re-forming the liquid films.

2.5.2 Emulsions

An emulsion is a dispersion of one liquid in a second, immiscible liquid. Emulsions are multiphase systems, even though they often look like they are just one phase. The phases in an emulsion are normally called the continuous phase and the disperse phase. Emulsion formed when oil is the dispersed phase and water is the continuous phase is known as oil in water emulsion **Fig. 2.5**, while those formed when water is the dispersed phase and oil is the continuous phase is known as oil in water emulsion **Fig. 2.6**.

When an emulsion is agitated, the droplet size becomes smaller. Mixing oil and water with some surfactants usually form an emulsion in which the individual droplets can be seen. The droplets formed by mixing are normally 100 to 500 μm in size, and are visible to the naked eye (1000 μm = 1 mm). By the use of a proper emulsion mixer it is possible to achieve a droplet size of 100 to 1000 nm (1000 nm = 1 μm).

In this research effort, the effects of foam and emulsion formed during two-phase gas-oil and three-phase gas-oil-water flow operations on CCGL performance was examined and documented.

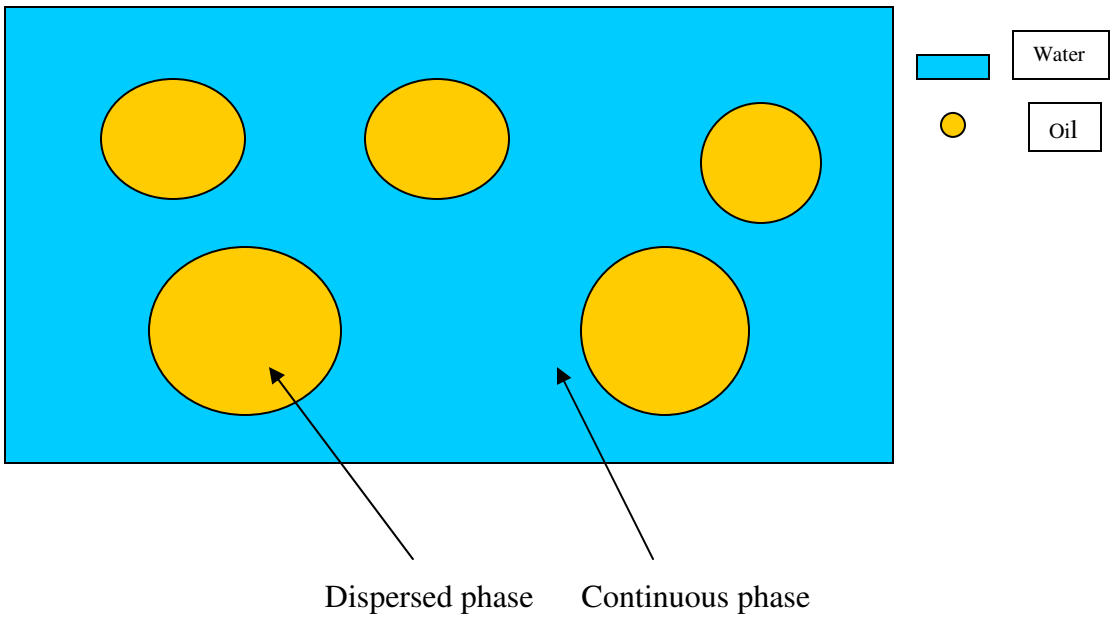

Fig. 2.5—Oil in water emulsion

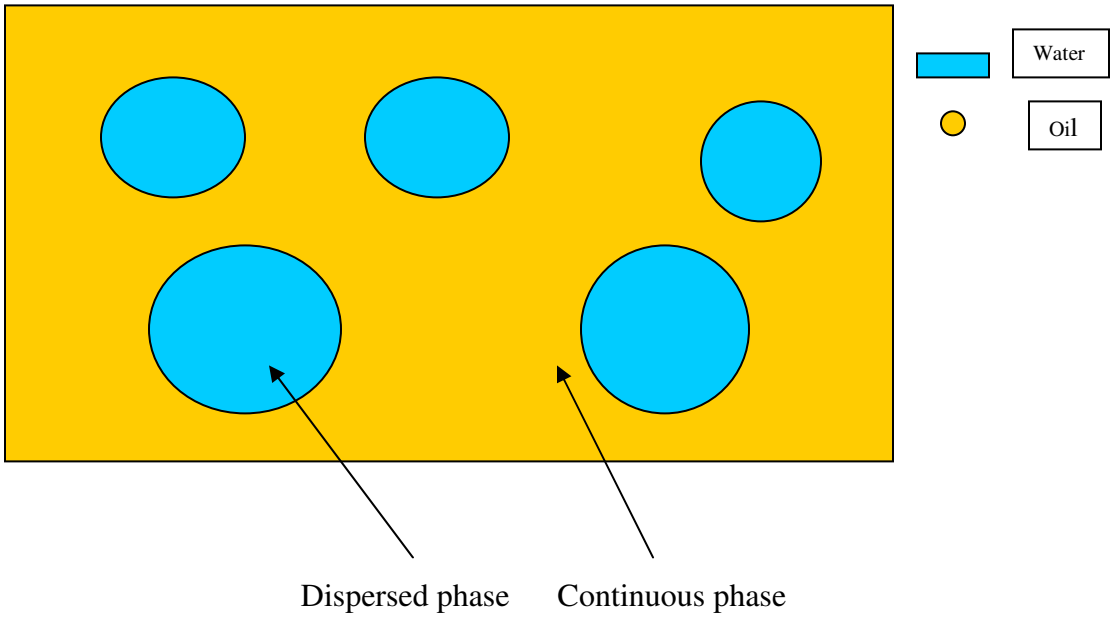

Fig. 2.6—Water in oil emulsion

CHAPTER III

EXPERIMENTAL PROGRAM

3.1 Test facility

The experimental two-phase flow loop consists of a metering section to measure the single-phase gas and liquid flow rates and a cylindrical cyclone test section, where all the experimental data are acquired **(Fig. 3.1).**

Fig. 3.1—CCGL separator test facilities with metering loop application.

3.1.1 CCGL test section

The test section consists of a cylindrical cyclone separator. The test section is divided into five parts:

- The inlet section adaptable to variable inlet slot sizes.
- The cylindrical cyclone body.
- The gas leg, which includes the liquid carry-over trap.
- The liquid leg with the gas carry-under trap.
- The recombination section.

3.1.2 Inlet-section

This experiment used variable inlet slots of three sizes **(Fig. 3.2)**, which are inlet spools with rectangular slot areas of 0.00434 ft^2 (No.1), and 0.00694 ft^2 (No.2). The third slot is the tangential inlet into the inlet section with an area of 0.03342 ft^2 (No.3).

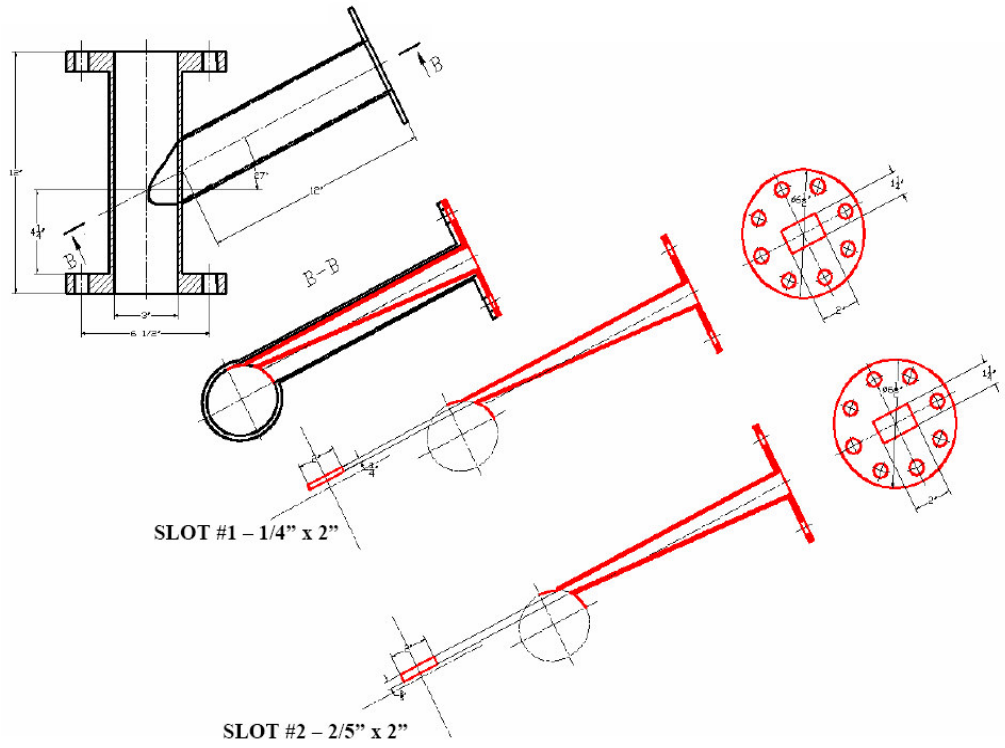

Fig. 3.2— Inlet-geometry and changeable inlet-slots will allow variation in flow conditions (Igho14)

3.1.3 Metering section

The metering section consists of two parallel, single-phase feeder lines for measuring the incoming single-phase gas and liquid flow rates. Air, which is supplied by an air compressor, is used as the gas phase. The gas flow rate into the loop is controlled by a regulating valve and metered by an elite series micromotion (ESM) coriolis meter. The liquid phase is oil and is supplied from a 5-barrel storage tank at atmospheric pressure and pumped to the liquid feeder line by a combination of two centrifugal pumps.

Similar to the gas phase, the liquid flow rate is controlled by a regulating valve and metered using 1½-in. Model D Micromotion meter. The single-phase gas and liquid streams are combined at the mixing tee and delivered to the test section. Check valves, located downstream of each feeder, is provided to prevent backflow. The two-phase mixture downstream of the test section is separated by a conventional separator. The gas is vented to the atmosphere and the liquid is returned to the storage tank to complete the cycle.

3.2 Experimental procedure

The overall test schematics proposed for this experimental work appears in **Figs. 3.3 and 3.4.** Oil, air, and water run in the flow loop; oil is supplied from a storage tank to the test area by progressive cavity pumps. Water is pumped into the loop from a water storage tank by centrifugal pumps. Variable frequency drives are applied to control oil and water rates. Air for the gas loop will come from a compressor, which is regulated with a needle control valve. Pressure transducers are located all around the test facility to provide the required pressure measurements.

All the streams are linked together at a mixing tee and the ensuing multiphase flow is fed into the separator. At the recombination points, the separated phases are combined and are allowed to flow back to a settling tank, where air is released into the atmosphere and the liquid phase is recirculated. The Elite Series Micromotion ½-in. coriolis meter is already in place to measure the gas rates, and a 1 ½-in. Model D Micromotion meter for both oil and water rates was not used for the experiment.

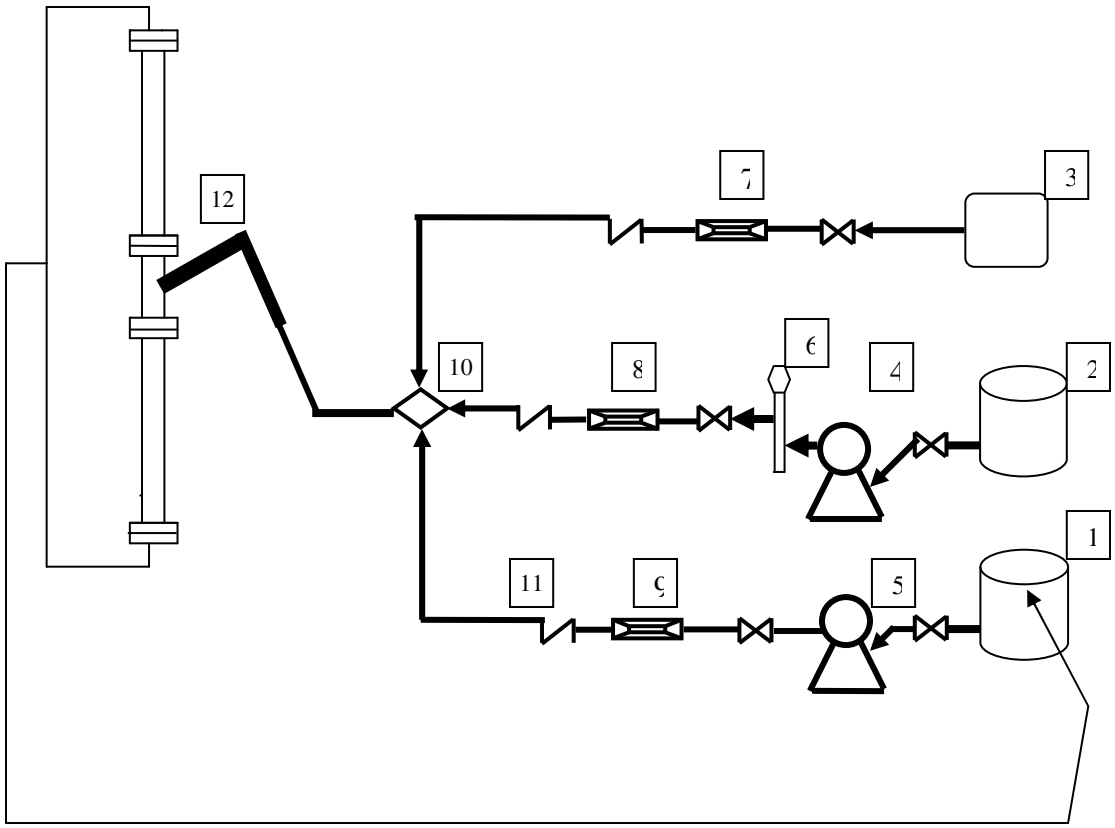

1 —Water storage tank

2 —Oil storage tank

3 —Air compressor

4 —Centrifugal pumps

5 —Progressive cavity pumps

6 —Water cut probe

7 —Air meter

8 —Liquid meter (1)

9 —Liquid meter (2)

10—Mixing tee

11—Check valve

12—CCGL

Fig. 3.4 —Test section will allow two-phase flow through the entire facility.

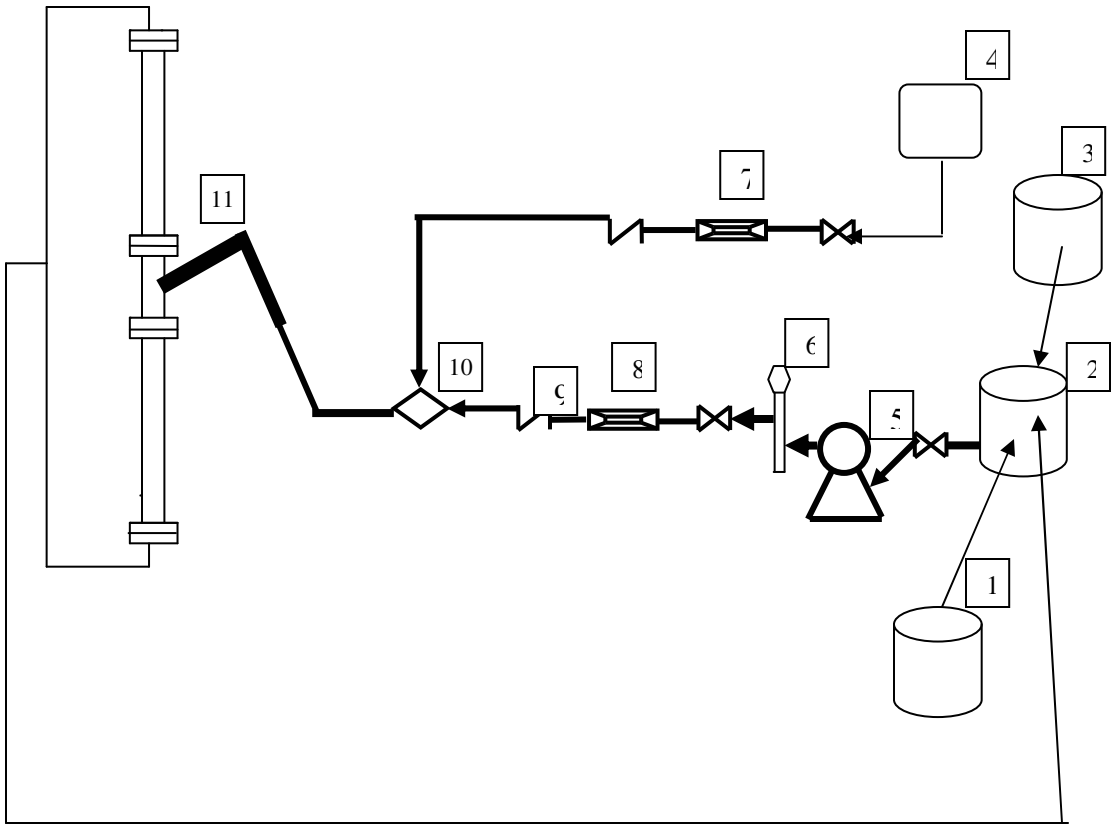

1 —Water storage tank

2 —liquid mixing tank

2 —Oil storage tank

4 —Air compressor

5 —Centrifugal pumps

6 —Water cut probe

7 —Air meter

8 —Liquid meter

9 —Check valve

10—Mixing tee

11—CCGL

Fig. 3.4 —Test section will allow three-phase flow through the entire facility

3.2.1 Data acquisition system

The average pressure of the cylindrical cyclone is measured by an absolute pressure transducer. The equilibrium liquid level (ELL) is estimated by sight gauge. Output signals from all measuring devices (pressure transducers, flow rate meters, temperature sensors, and density/water cut probe) terminates at a central panel connected to the computer by the use of an analog to digital converter. A NI-DAQ data-acquisition system with Lab View 8.0 from National Instrument as the graphical-user interface is used to acquire data from the measuring devices. The sampling frequency is fixed at 1 Hz .When a steady state condition is attained; a mean of data recorded for a run, usually about 3 minutes is taken as the final measurement.

3.2.2 ZNLF test procedure and data acquisition

The method adopted to acquire data for zero-net liquid flow (ZNLF) is as follows, the liquid section outlet is completely shut and then the CCGL separator is gradually filled to the gas outlet with test liquids first water with density of 1.0 g/cc or 0.834 ppg, then oil (Conono LVT 200) with density of 0.7 g/cc or 0.582 ppg and later oil and water mixture. The pumps are turned off to make volumetric liquid flow rate through the separator zero. Gas is allowed to flow through the static liquid column until no liquid carry over (equilibrium conditions) .The gas rate is recorded, and then gas flow is shut-off to report the equilibrium liquid level of the upper column of the separator. This procedure is repeated for different gas rates until total liquid blow out is obtained above the separator inlet. This test is repeated for the each inlet-slot geometry and recombination point.

3.2.3 LCO test procedure and data acquisition

For the LCO tests, air flow rate is maintained at a constant value; liquid flow rate is gradually increased until the initiation of LCO. While, the control valve on the gas exit of the separator is adjusted constantly to a set pressure at the existing liquid rate into the separator. This process is repeated for other gas rates until the operational envelope is defined. The valve at the liquid leg was left fully opened through out the test process. Three different constant separator pressures of 3, 7, and 9 psig were employed for these

tests. The whole test procedure was carried out initially with water as the liquid medium, then oil and later oil and water mixture. The effects of the changeable inlet slots were also examined at constant separator pressures.

The tests for the gas carry-under were not carried out, this is due to the inefficient gas trapping device installed with the test facility. The results of all these experimental investigations are reported in chapters four and five.

CHAPTER IV

THREE-PHASE FLOW CCGL SEPARATOR OPERATIONS

4.1 Zero net liquid flow for two-phase system

One of the essential operational features of the CCGL separator is the zero net liquid flow (ZNLF).The ZNLF is the maximum gas flow rate that can be tolerated by the separator before the onset of liquid carry-over. This phenomena occurs whenever the equilibrium liquid level (ELL) is located above the inlet, during ZNLF, the liquid phase either slugs or churns through the upper part of the separator column without any liquid carry over.

ZNLF is affected by several factors such as the design of the separator, flow pattern in the separator, and the property of the mixture. In the upper part of separator two-phase flow is observed, with only the gas phase flowing out from the top. The ratio of the in-situ liquid volume to the volume of the pipe in the upper part of the separator is known as the zero-net liquid holdup.

A proper estimate of ZNLF holdup is important in defining the Liquid carry-over operational envelope for compact separators. Also, it is necessary to know the liquid holdup to determine mixture density, effective viscosity and the actual gas and liquid velocities. The expression for ZNLF holdup, H_{L0} , can be derived from the definition of slip between the gas and liquid phases, v_S;

$$v_S = v_G - v_L = \frac{v_{SG}}{(1-H_L)} - \frac{v_{SL}}{H_L} \tag{4.1}$$

During ZNLF conditions, the superficial liquid velocity is zero. Therefore, the gas slip velocity is given as

$$v_{Go} = \frac{v_{SG}}{(1-H_L)} \tag{4.2}$$

And rearranging,

$$H_{Lo} = 1 - \frac{v_{SG}}{v_{Go}} \tag{4.3}$$

This project was done at low-pressure conditions, the low pressure ZNLF holdup correlations were applied for analysis. The two-phase hydrodynamic model by Arpandi for predicting the LCO operational envelope combines equilibrium liquid level predictions with ZNLF holdup correlations to determine the LCO operational efficiency.

From this model, H_{L0}, can be calculated from

$$H_{Lo} = \left[\frac{v_{SG}}{(1 - H_L)}\right] * \left[1 - \frac{L_d}{L_{gi}}\right] \tag{4.4}$$

The factor (1-L_d/L_{gi}) accounts for the holdup only in the upper part of the separator. The ZNLF gas velocity as a function of Taylor bubble rise velocity is

$$v_{Go} = C_o v_{SG} + 0.35\sqrt{g d_{sep}\left[\frac{\rho_l - \rho_g}{\rho_l}\right]} \tag{4.5}$$

Where L_d is estimated from

$$L_d = \frac{1}{\frac{2g_c}{v_{SG}^{\ 2}} - \frac{C_d}{2}\left(\rho_g v_{SG}\right)^2 * \frac{3}{32\rho_l \sigma g_c}} \tag{4.6}$$

4.1.1 Effects of inlet-slot geometry and recombination points

The results of ZNLF holdup for three inlet-slot configurations for the air-water system are presented in **Fig. 4.1**. This data was obtained at three recombination at points #1, #2, and, #3 located at distances 2.58ft, 3.39ft, and 4.28 ft from the bottom of the CCGL separator **Fig. 4.3-4.5**. From these plots, varying the inlet area through the use of

adjustable inlet slots has no effects on the ZNLF holdup. Also, the recombination points have no noticeable impacts on the results; this could be attributed to the fact that only gas is flowing out of the system to the atmosphere.

Therefore, the G-force required for separation achievable through the use of inlet-slot configurations does not affect the ZNLF holdup property of the CCGL separator. Similar results were obtained for the air-oil system for slot configurations **Fig. 4.2** and **Figs. 4.6-4.8** for the recombination points.

These results and conclusions remain true only if the length of the upper gas section above the inlet, L_{gl}, is properly designed for churn flow pattern to be established prior to the onset of liquid carry-over (LCO).

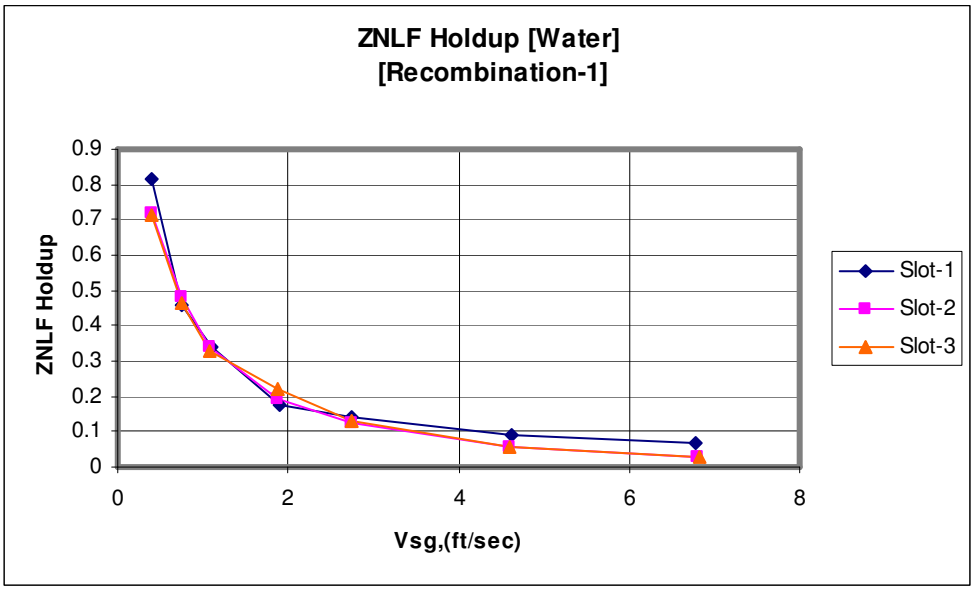

Fig. 4.1— ZNLF holdup profile for water using different slot geometry.

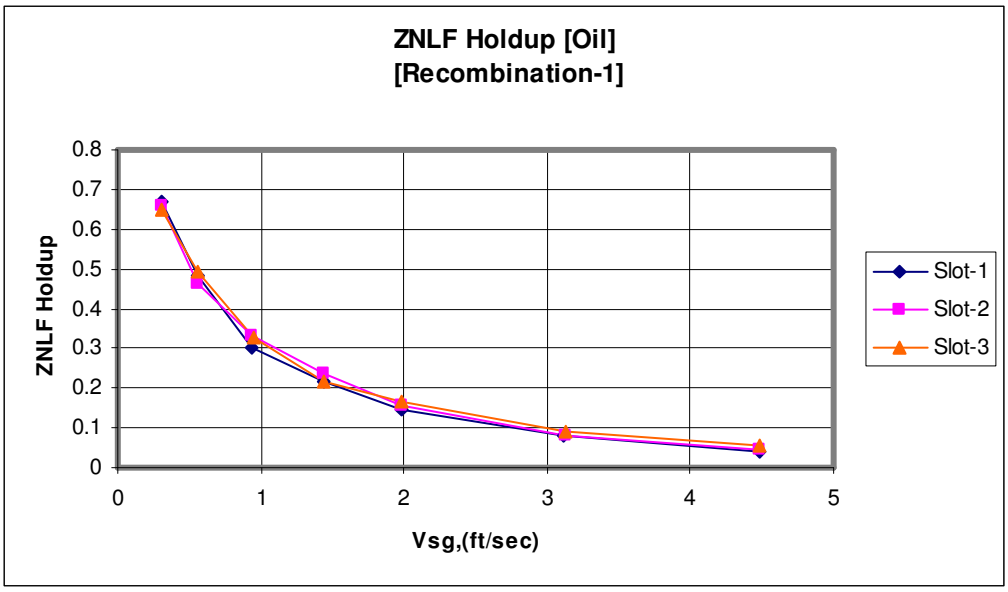

Fig. 4.2— ZNLF holdup profile for oil using different slot geometry.

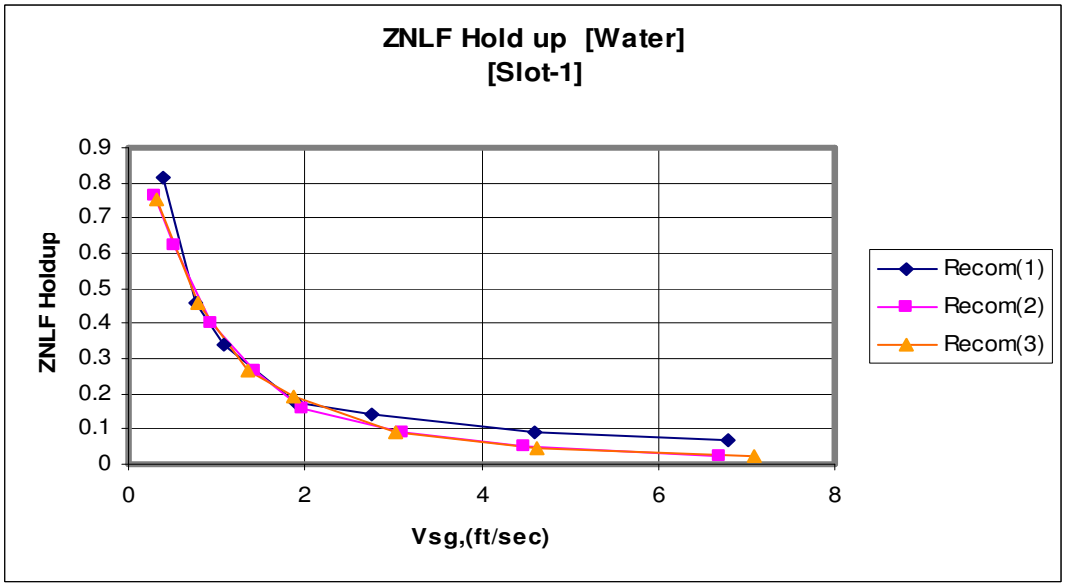

Fig. 4.3— ZNLF holdup profile for slot-1 at three recombination points.

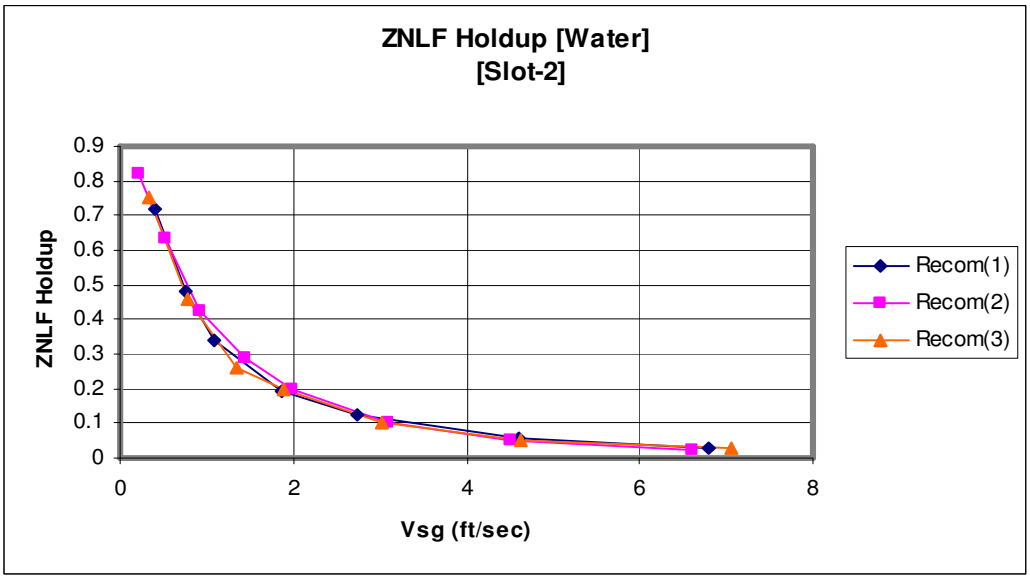

Fig. 4.4— ZNLF holdup profile for slot-2 at three recombination points.

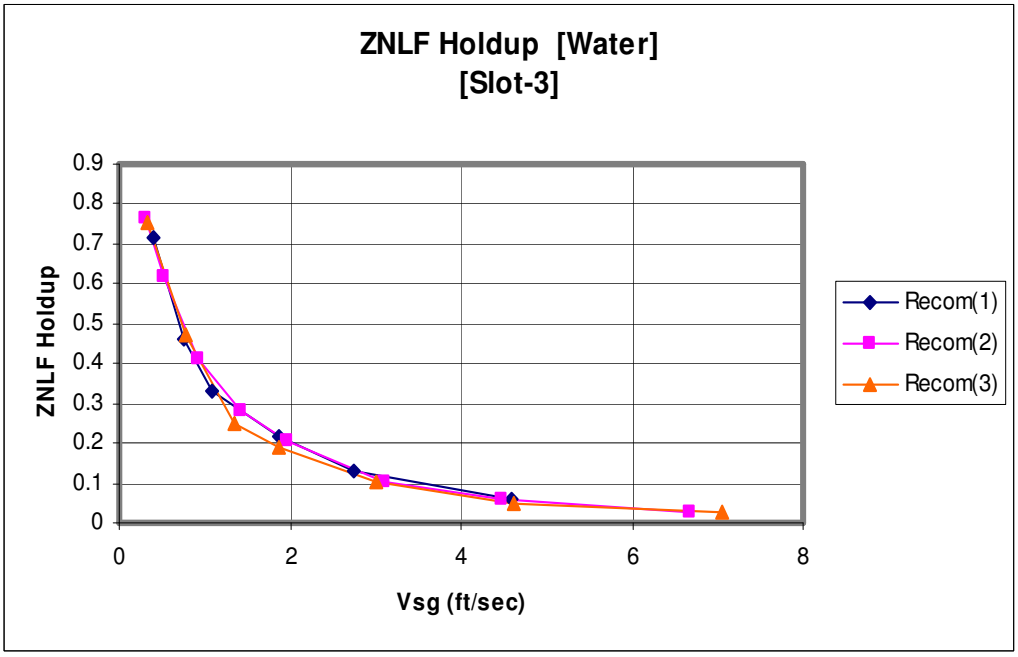

Fig. 4.5— ZNLF holdup profile for slot-3 at three recombination points.

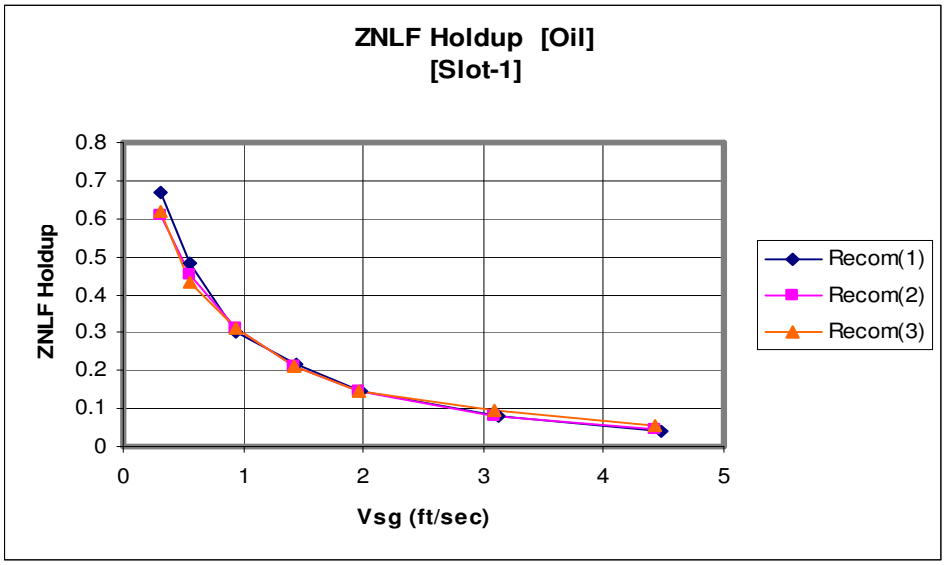

Fig. 4.6—ZNLF holdup profile for slot-1 at three recombination points.

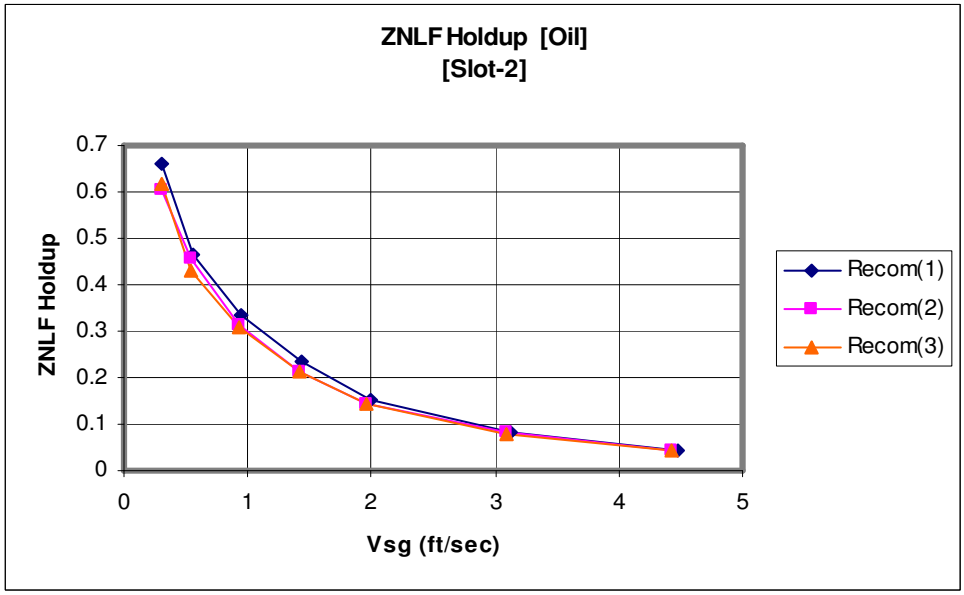

Fig. 4.7—ZNLF holdup profile for slot-2 at three recombination points.

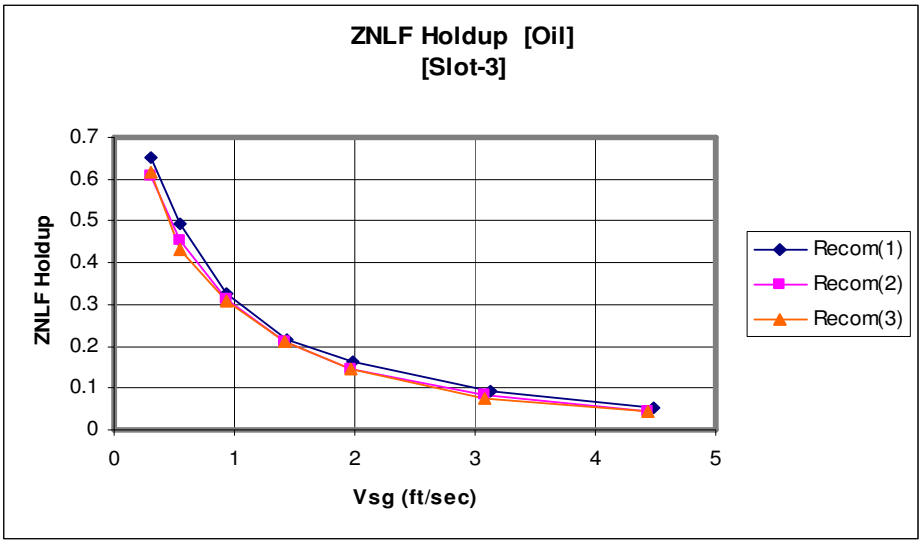

Fig. 4.8—ZNLF holdup profile for slot-3 at three recombination points.

4.1.2 Effects of liquid density on ZNLF holdup

The plots of the effects of changes in liquid density on ZNLF holdup are presented in **Figs. 4.9-4.11**. The ZNLF holdup decreases with increase in gas flow rate for both water and oil. These plots indicate ZNLF holdup is a function of the superficial gas velocity. Also, as the density increases from 0.7g/cc (0.542ppg) for oil to 1.0g/cc(0.834ppg) for water, the ZNLF holdup is observed to increase.

Fig. 4.12 shows a comparison of the ZNLF holdups for liquids of different densities from An *et al.*,[7] for a vertical pipe section and pressure maintained at 25 psig with the ZNLF holdup obtained in this work using the CCGL separator maintained at 3 psig. An examination of the figure revealed very similar trend in the ZNLF curves, the only difference is that higher values of ZNLF holdup are seen in An's work, this would be expected since ZNLF Holdup is a function of pressure.

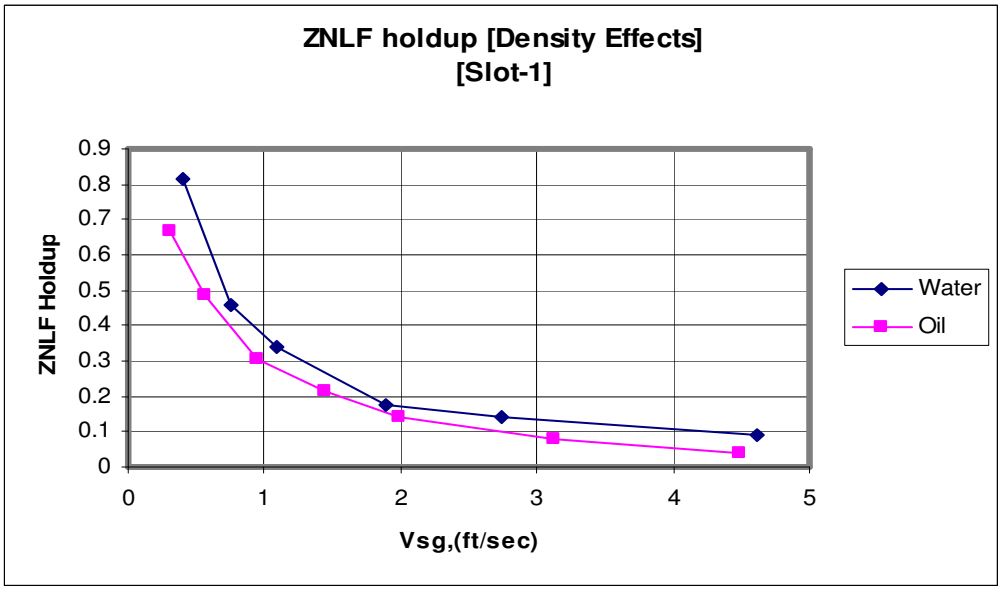

Fig. 4.9—Effects of density on ZNLF holdup using slot-1.

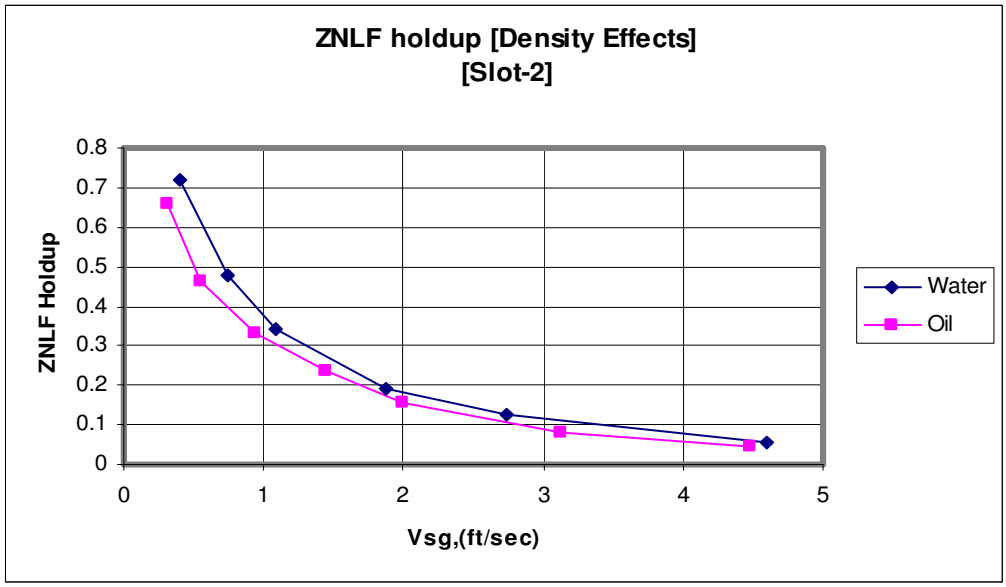

Fig. 4.10—Effects of density on ZNLF holdup using slot-2.

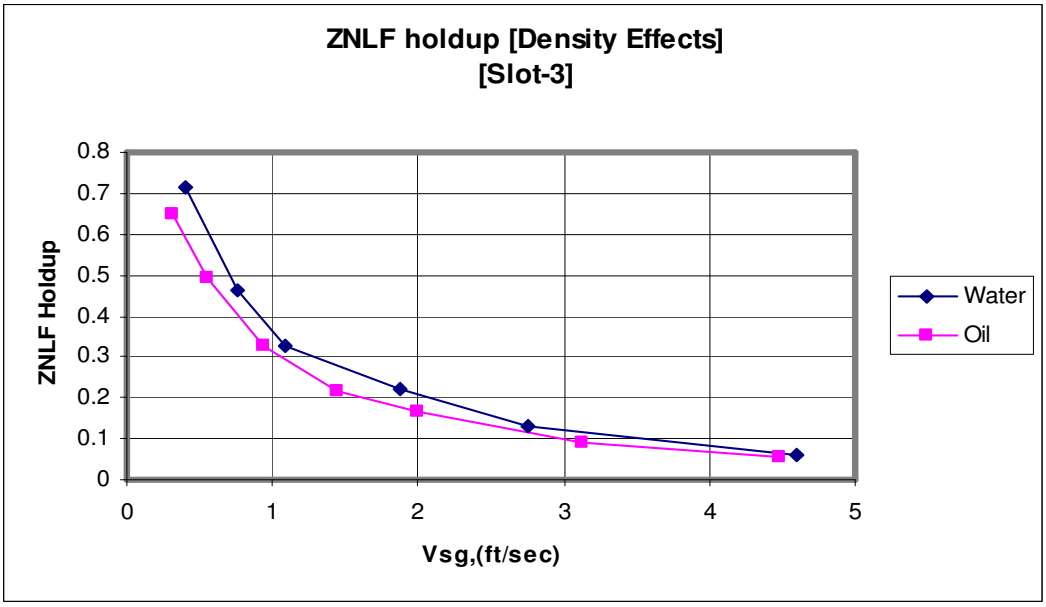

Fig. 4.11—Effects of density on ZNLF holdup using slot-3.

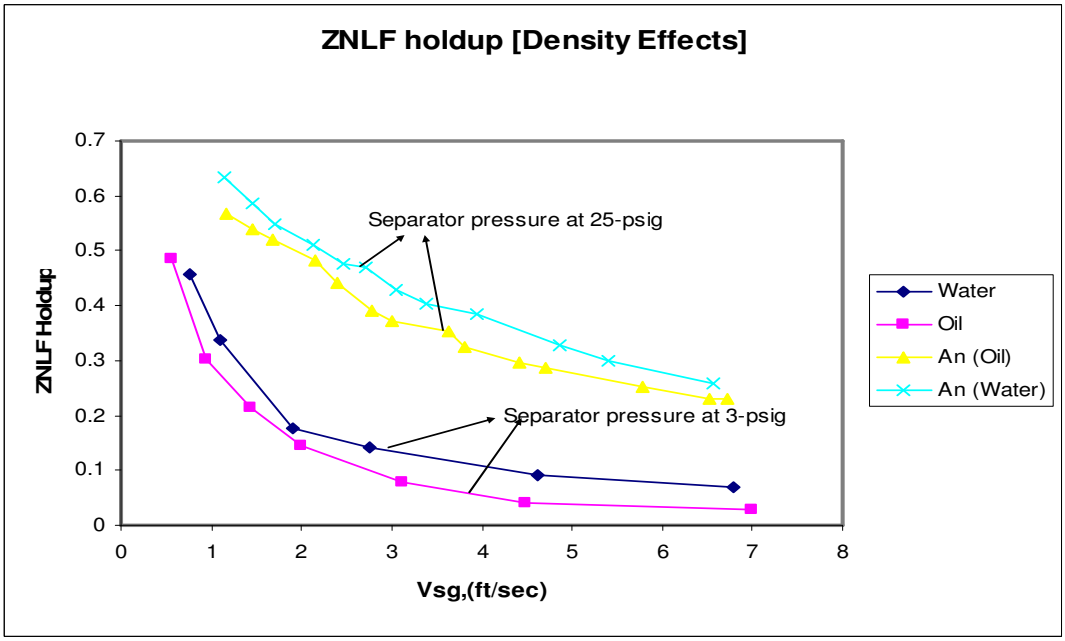

Fig. 4.12—Comparison of ZNLF holdup with previous work for density effects

4.2 LCO operational envelope

4.2.1 The effects of foam formation on LCO operational envelope

The effect of foam formation on LCO performance of the CCGL separator during two phase flow operation was investigated using the slot configurations at different separator pressures. This was achieved by replacing water with oil of high foaming tendencies. Separator pressures were obtained by regulating the choke valve on the gas leg.

Many works have indicated significant improvement in LCO operational envelope through the use of adjustable inlet-slot configurations and by recombining the gas and liquid streams at the lowest recombination point. The results from this project showed a deviation from the reported improvement in LCO performance when liquids with high foam formation tendencies were used as the liquid phase. **Figs. 4.13-15** show a wide variation in the LCO operational envelope when light oil of high foam property was the liquid phase.

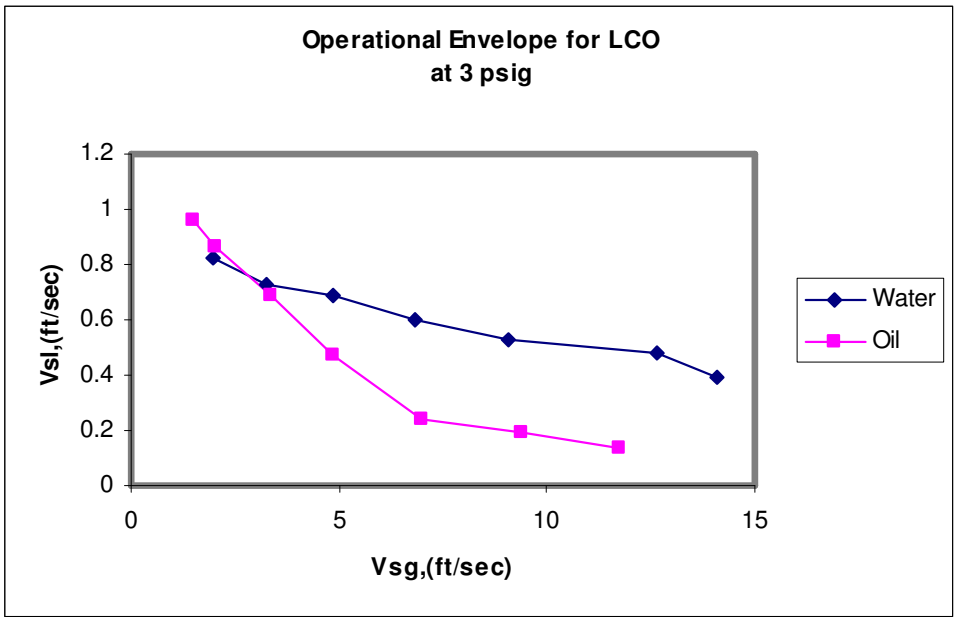

Fig. 4.13—Effects of foam formation on LCO at 3-psig

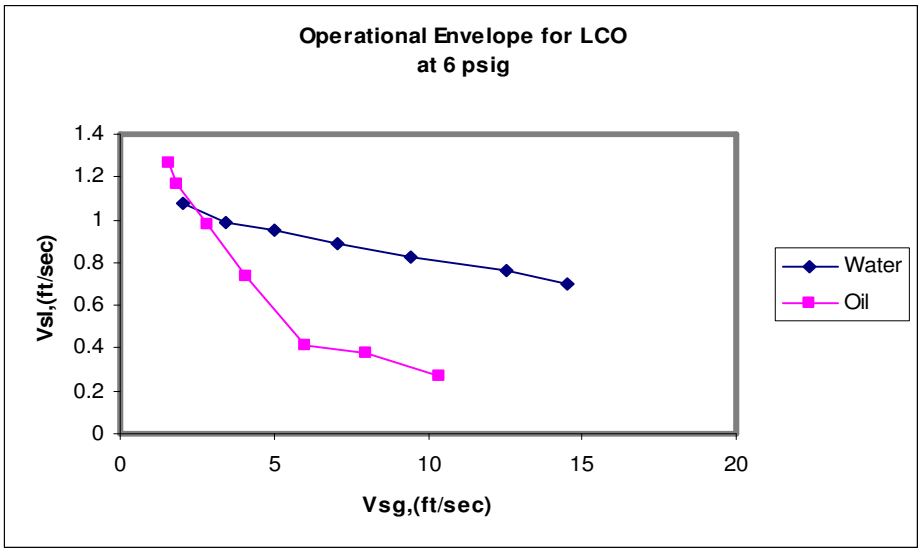

Fig. 4.14—Effects of foam formation on LCO at 6-psig

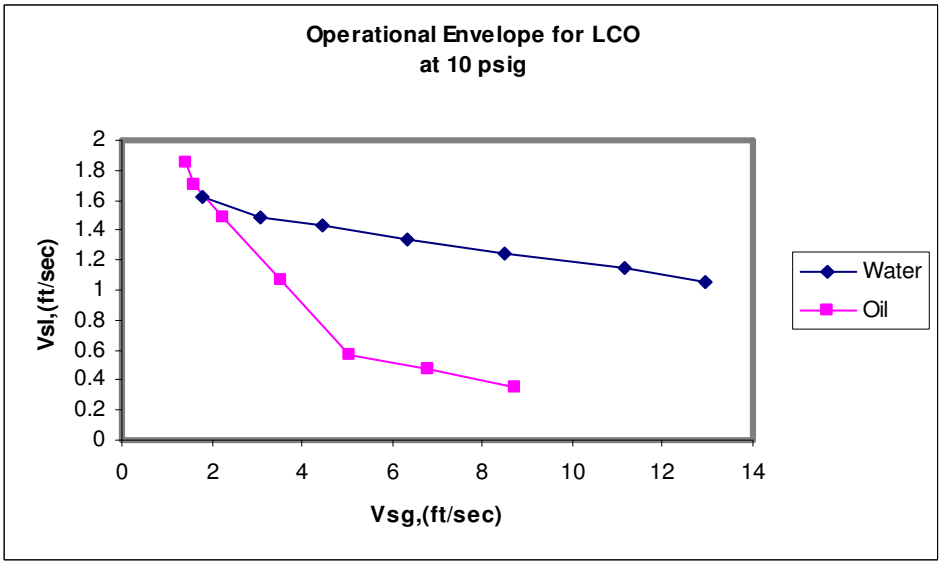

Fig. 4.15—Effects of foam formation on LCO at 10-psig

It can be seen clearly that at high liquid rates and low gas rates irrespective of the pressure in the separator, the separator operates as would be expected in bubble flow region where only the effects of density and viscosity of the liquid medium are the dominant factors affecting its performance. As the gas rate increases, the LCO operational envelope reduces very rapidly when oil is the liquid phase. This is due to the formation of foam bubbles as the oil churns up and down the upper part of the separator column leading to early initiation of LCO.

4.2.2 The effects of pressure on foam formation and LCO operational envelope

Although as the pressure within the separator increases the LCO operational envelope increases, but the curves in Fig. 4.15 becomes wider apart as a result of severe foaming causing early onset of LCO. A close observation of the complex flow dynamics in the separator reveals that as the gas rate increases the foam bubbles are pushed over to the top of the gas section by the incoming gas, and as the bubbles travel through the gas leg encountering a low pressure region, they collapse into two distinct phases.

4.2.3 Minimizing foaming to improve CCGL separator performance

In order to reduce foam generation during separation in the CCGL, the separator can be operated at low pressures by adjusting the needle valve of the gas leg exit of the CCGL separator, as this will cause gas entrapped within the foam to expand and resulting in the collapse of the foam bubbles. Since most operations in the field are usually at high pressure, this method may not be feasible. Another option is to design the upper section of the CCGL separator in such a way as to allow for enough time for foam formed during separation to settle. Also this may not be feasible for very high rate wells. In my opinion adding antifoaming or defoaming agents to the multiphase mixture will be the most suitable option as this will reduce if not eliminate any foaming prior to separation in the CCGL separator.

CHAPTER V

THREE-PHASE FLOW CCGL SEPARATOR OPERATIONS

5.1 Overview of three-phase flow CCGL separators

Separation technique for gas-oil-water in the petroleum industry has been done by the use of conventional vessel-type separator. As the drive towards attaining significant cost reduction especially in offshore field production is receiving tremendous attention, the industry is rigorously searching for alternative technologies that can help achieve this goal. One of such novel technologies is the compact separator, which is low cost and low weight. But the lack of complete understanding of the complex hydrodynamic flow situations has limited its widespread use. Three-phase flow comprising of oil, water, and gas is the common multiphase feed into the CCGL separator in many production field operations. And as such, it has been reported in some publications such as Zhang *et al*[23] that three-phase flow behavior such as liquid holdup and pressure gradient varies differently from those of two-phase flow. At this point, it is still very difficult to develop a reliable model that can adequately predict three-phase flow system in vertical pipe section as it is the case with the cyclone separator; therefore, experimental investigation is needed to verify separator performance during three-phase flow.

In gas-oil–water three phase pipe flows, the phase distributions and hydrodynamics are described based on two distinct criteria: gas-liquid flow pattern and oil-water mixing status. The three-phase flow is treated as gas-liquid two phase flow if the two liquids are fully mixed. This may be true for vertical and steeply inclined flows, and slug and annular flows at high flow rates. The physical properties of the liquid mixture can be calculated based on the fractions and the individual physical properties of the two liquid.

The other case is to treat three-phase flow as a stratified flow with gas on the top, oil in the middle and water at the bottom. This can be done for immiscible liquids flowing in horizontal or slightly inclined pipes with low gas, oil, and water rates. Most three-phase flows fall between these two extremes[24].

In this investigation, the first case was considered that is the three-phase flow in the compact cyclone separator was treated as gas-liquid two phase since the separator is of a vertical configuration and the liquid phases are fully mixed.

Again, by the use of the two-phase model in chapter IV we can rewrite an expression for ZNLF holdup for a three-phase flow system, H_{Lomix} , can be derived from the definition of slip between the gas and liquid phases, v_S;

$$\upsilon_S = \upsilon_G - \upsilon_{Lmix} = \frac{\upsilon_{SG}}{(1 - H_{Lmix})} - \frac{\upsilon_{SLmix}}{H_{Lmix}} \tag{5.1}$$

Also for ZNLF conditions, the superficial liquid mixture velocity is zero. Therefore, the gas slip velocity is given as

$$\upsilon_{Go} = \frac{\upsilon_{SG}}{(1 - H_{Lomix})} \tag{5.2}$$

Rearranging,

$$H_{Lomix} = 1 - \frac{\upsilon_{SG}}{\upsilon_{Go}} \tag{5.3}$$

For low pressure ZNLF holdup correlations, since this investigation was done at low-pressure and by the use of Arpandi's model for predicting the LCO, H_{L0mix} for the oil-water mixture is calculated from

$$H_{Lomix} = \left[\frac{\upsilon_{SG}}{(1 - H_{Lmix})}\right] * \left[1 - \frac{L_d}{L_{gi}}\right] \tag{5.4}$$

The ZNLF gas velocity is

$$v_{Go} = C_o v_{SG} + 0.35\sqrt{g d_{sep}\left[\frac{\rho_{lmix} - \rho_g}{\rho_{lmix}}\right]} \tag{5.5}$$

Where

$$\rho_{lmix} = h_{o\tan k}\rho_o + h_{w\tan k}\rho_w \tag{5.6}$$

L_d is calculated by

$$L_d = \frac{1}{\frac{2g_c}{v_{SG}^{\ 2}} - \frac{C_{dmix}}{2}\left(\rho_g v_{SG}\right)^2 * \frac{3}{32\rho_{lmix}\sigma_{mix}\, g_c}} \tag{5.7}$$

5.2 Three-phase flow performance of the CCGL separators

This research has focused primarily on the effect of foam and emulsions on separator properties such ZNLF and LCO performance of the CCGL separator during three-phase flow operation. This was done by mixing a certain fraction of water and oil thoroughly in a mixing tank. Then, the ensuing oil-water mixture is allowed to flow into the test facility for the ZNLF and LCO experiments. The whole procedure was repeated several times with different fractions of oil-water mixture. The following sections report the outcome of these experimental investigations.

5.2.1 Three-phase flow performance of CCGL under ZNLF operations

Figure 5.1 shows a summary of the results obtained for ZNLF holdup under a range of water cut at low separator pressures. At a range of water-cut of 10% to 90% there is little or no variation in the values of the ZNLF holdup for a given superficial gas velocity.

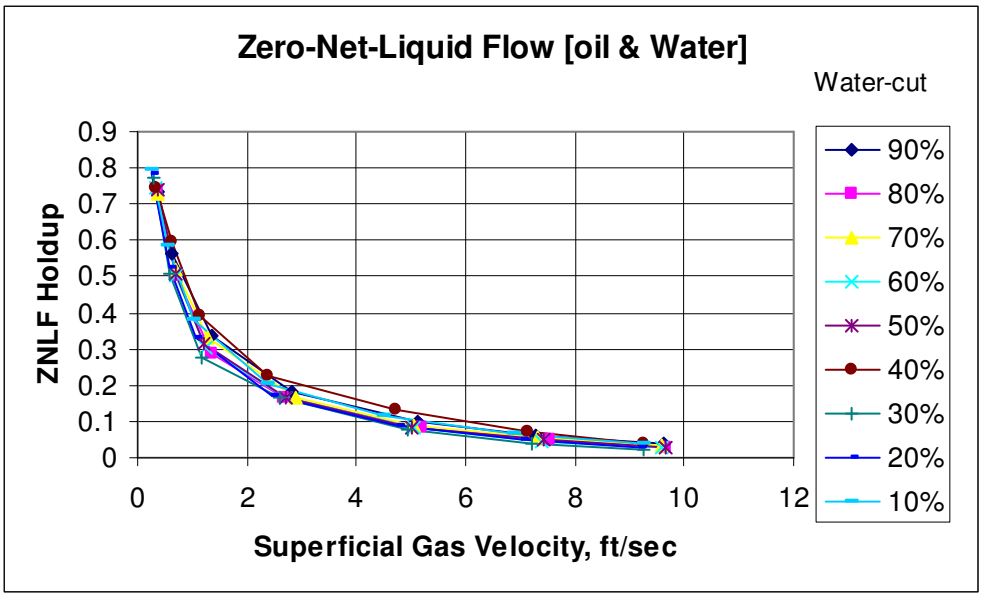

Fig. 5.1—Effect of water-cut on ZNLF holdup

5.2.2 Three-phase flow LCO operational envelope of CCGL separators

The results of the experimental investigation for gas-oil-water three-phase flow LCO separator operations are presented in **Figs. 5.2-5.4**. A close observation of the plots showed that at low gas rates in bubble region irrespective of the water-cut of the multiphase stream, the separator performance is very good. However as the water-cut continue to decrease as we approach churn/slug flow region, separator performance became very poor as there was early initiation of LCO conditions. This situation could be attributable to severe foaming due to oil becoming the dominant liquid in the liquid mixture.

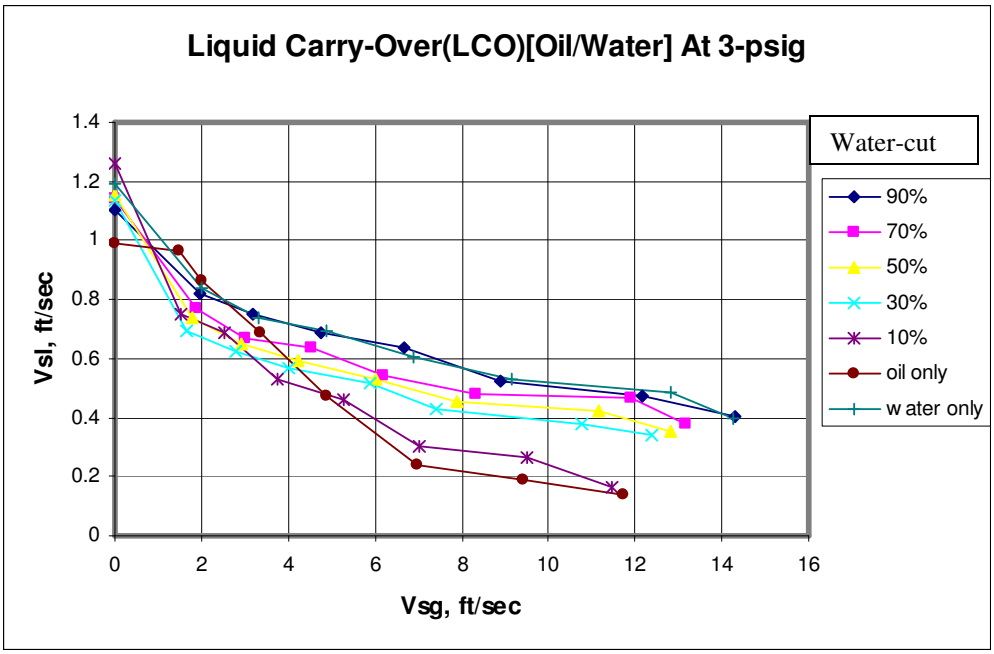

Fig. 5.2—Effect of water-cut on LCO performance of CCGL at 3-psig

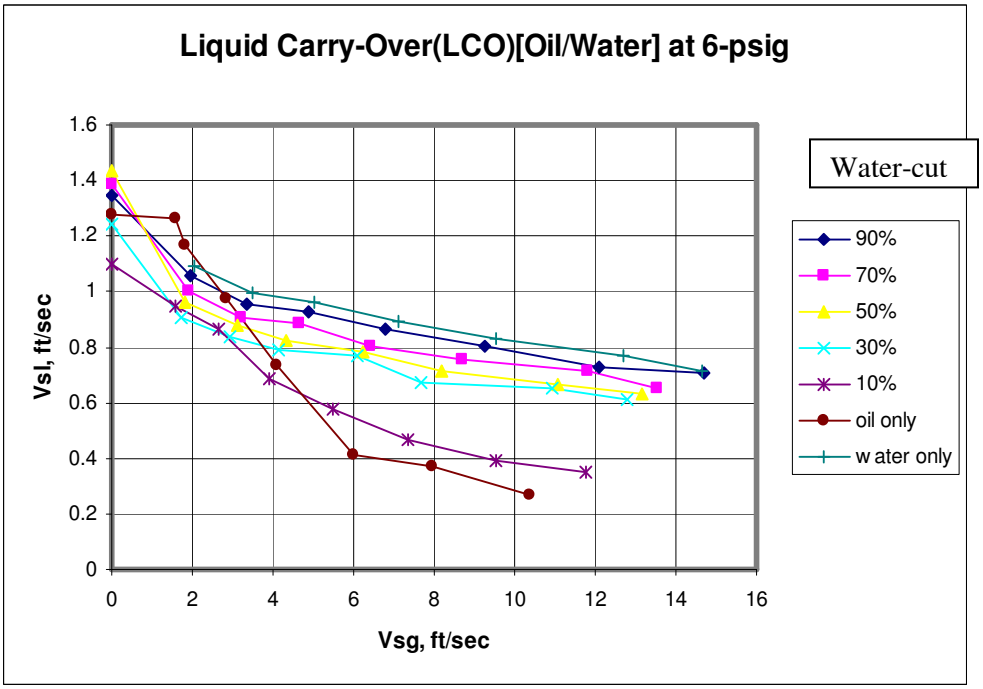

Fig. 5.3—Effect of water-cut on LCO performance of CCGL at 6-psig

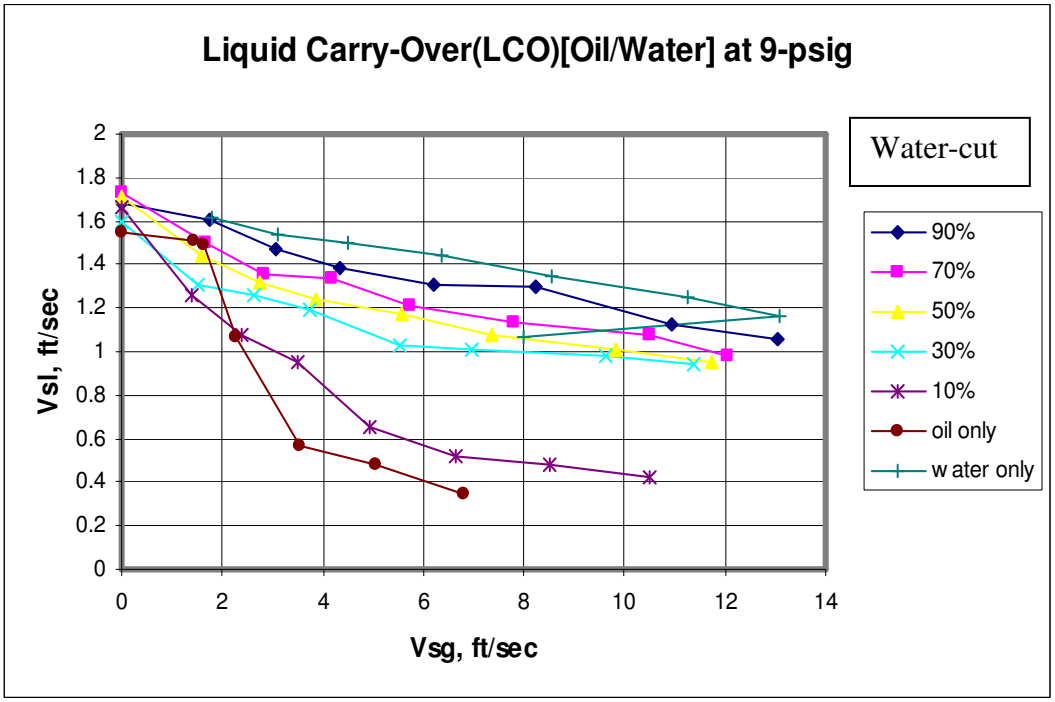

Fig. 5.4—Effects of water-cut on LCO performance of CCGL at 9-psig

5.2.3 The effects of inlet area on LCO separator performance

The effects of varying the inlet area through the use of sleeves are shown in **Figs. 5.5-5.7.** The areas provided by these spools are 0.00434 ft^2 (No.1), and 0.00694 ft^2 (No.2). and the third slot is the tangential inlet section of the CCGL with an area of 0.03342 ft^2 (No.3). From Figs. 5.5 and 5.6, at high water-cut the impacts of any change in the inlet area on the LCO curves are not noticeable, but at low water cut in Fig 5.7 particularly in the bubble flow region, a slight improvement in LCO performance of the CCGL was observed. This is as a result of the fact severe foaming has not been initiated as was the case at high gas rate in the churn/slug regime where varying the inlet area has negligible influence on LCO separator performance.

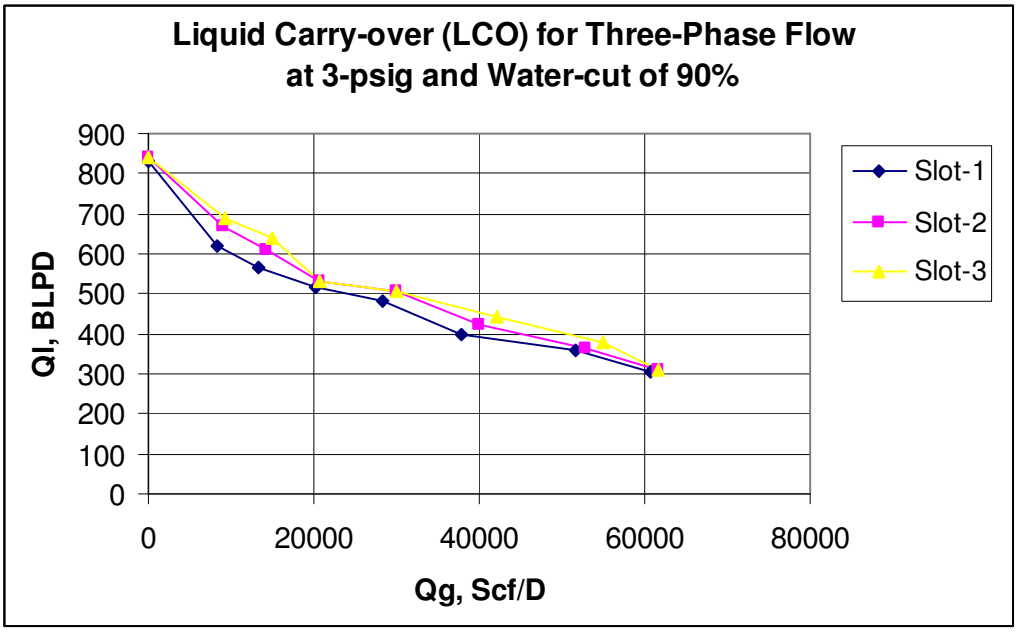

Fig. 5.5 —Effects of inlet-slot area on three-phase flow CCGL operations with 90% water-cut

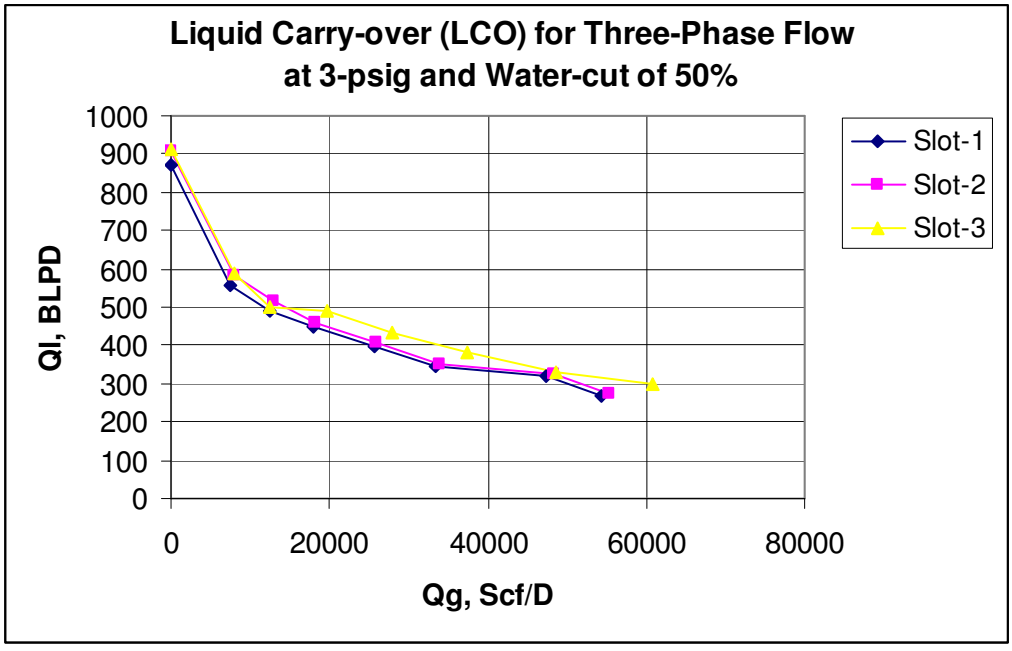

Fig.5.6 —Effects of inlet-slot area on three-phase flow CCGL operations with 50% water-cut

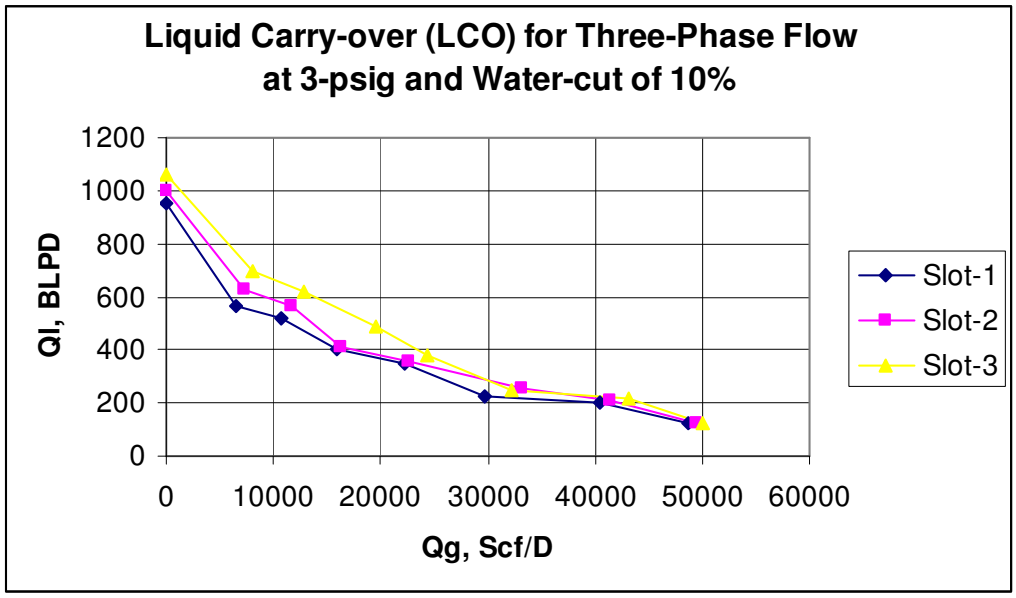

Fig.5.7 —Effects of inlet-slot area on three-phase flow CCGL operations with 10% water-cut

CHAPTER VI

CONCLUSIONS AND RECOMMENDATIONS

6.1 Conclusions

From the results of this experimental investigation the following conclusions were reached.

1. ZNLF Holdup is a strong function of the superficial gas velocity. The ZNLF Holdup decreases with increase in gas flow rate.
2. Density increases from 0.7g/cc (oil) to 1.0g/cc (water) leads to increase in ZNLF Holdup.
3. Varying the inlet area has no effects on the ZNLF holdup. The recombination points have no noticeable impact .The G-force required for separation does not affect the ZNLF holdup.
4. As gas rate increases, the LCO operational envelope reduces very rapidly when oil is the liquid phase. Similar results were obtained at low water-cut of about 30 % during three-phase flow operations of the CCGL separator.
5. Varying the inlet-slot size has negligible influence on the LCO performance of the CCGL separator.
6. Formation of foam bubbles causes early initiation of LCO and as a result there is a significant reduction in LCO operational envelope of the CCGL separators.
7. The use of antifoaming agents or defoamers is needed to reduce the effect of foaming on LCO efficiency of the CCGL separator.

It has been clearly demonstrated in these efforts that foam generation during CCGL operations can have a severe impact on its performance. From the results of the experimental investigation on ZNLF and LCO separator performance, a proper design of the CCGL separator should incorporate a correction of existing design models to account for foam effects.

6.2 Recommendations

The following recommendations are made based on the results of this research.

1. An efficient gas trapping device needs to be provided for the test loop to investigate the GCU performance of the CCGL separator under three-phase flow conditions.
2. ZNLF and LCO tests at higher gas and liquid flow rates are needed to check separator response under three-phase flow situations.
3. The effects of fluid properties such as tendencies to foam and emulsion formation on compact separators should be further investigated using foamy heavy oil as found in field operations.
4. Design of a modular CCGL separator inlet section that will enable easy automated slot-size variation for large scale field operations
5. Tests should be conducted to check separator performance under three-phase flow at higher pressures as could be found in field operations.

NOMENCLATURE

A_{inlet} = inlet slot cross-sectional area

C_0 = flow coefficient

C_d = drag coefficient

C_{dmix} = drag coefficient of mixture

d_{sep} = internal diameter of separator

g = acceleration due to gravity

h_{osep} = oil volume fraction in CCGL separator

h_{wsep} = water volume fraction in CCGL separator

h_{otank} =oil volume fraction in mixing tank

h_{wtank} = water volume fraction in mixing tank

H_L = liquid holdup

H_{Lo} = ZNLF holdup

H_{Lomix} = ZNLF holdup of liquid mixture

K = gas expansion/compression parameter

L_{gl} = length of separator gas-leg

L_d = droplet region length

M_R = air mass rate

P = pressure

$P_{in\text{-}situ}$ = pressure at in-situ condition

Q_{g_insitu} = in-situ gas volumetric flow rate

Q_G = gas volumetric flow rate

Q_l = liquid volumetric flow rate

Q_{lmix} = liquid mixture volumetric flow rate

r = radius of separator

T = temperature

v_{SL} = superficial liquid velocity

v_{SG} = superficial gas velocity

v_{mr} = mixture velocity

v_s = slip velocity

v_G = gas velocity

v_{Go} = ZNLF gas velocity

v_{g_insitu} = in-situ gas velocity

v_L = liquid velocity

V_t = terminal settling velocity

α = angle of inclination of tangential inlet to the horizontal

ρ_o = oil density

ρ_w = water density

ρ_{lmix} = density of liquid mixture

ρ_g = gas density

σ = liquid surface tension

σ_{mix} = liquid surface tension

z = compressibility factor

REFERENCES

1. Erdal, F., Shirazi, S., Shoham, O., and Kouba, G.: "CFD Simulation of Single-Phase and Two-Phase in Gas-Liquid Cylindrical Cyclone Separators," paper SPE 36645 presented at the 1996 SPE Annual Technical Conference and Exhibition, Denver, 6-9 October.

2. Motta, B., Erdal, F., Shirazi, S., Shoham, O. and Rhyne, L.: "Simulation of Single-Phase and Two-Phase Flow in Gas-Liquid Cylindrical Cyclone Separators," ASME Summer Meeting, Fluid Eng. Division, Vancouver, Canada (1997).

3. Arpandi, I., Joshi, A., Shoham, O., Shirazi, S., and Kouba, G et al.: "Hydrodynamics of Two-Phase Flow in Gas-Liquid Cylindrical Cyclone Separators," paper SPE 30683 presented at the 1995 SPE Annual Technical Conference and Exhibition, Dallas, 22-26 October.

4. Mohan, R., Wang, S., Shoham, O., and Kouba, G.: "Design and Performance of Passive Control System for Gas-Liquid Cylindrical Cyclone Separators," *ASME J. Energy Resources Technology* (March 1998) **120**, No.1, 49.

5. Gomez, L., Moham, R., Shoham, O., and Kouba, G.: "Enhanced Mechanistic Model and Field Application Design of Gas-Liquid Cylindrical Cyclone Separator," paper SPE 49174 presented at the 1998 SPE 73rd Annual Technical Conference and Exhibition, New Orleans, 27-30 September.

6. Kouba, G.E., Shoham, O., and Shirazi, S.: ''Design and Performance of Gas-Liquid Cylindrical Cyclone Separators,'' *Proc.*, BHR Group Seventh Intl. Meeting on Multiphase Flow, Cannes, France (June 1995) 307.

7. An, H., Langlinais, J.P., and Scott, S.L.: "Effects of Density and Viscosity in Vertical Zero Net Liquid Flow," paper presented at the ASME- ETCE 2000 Production Technology Symposium, New Orleans, Louisiana; *ASME J. of Energy Resources Tech.*, (June 2000) **122**, 49-55.

8. Duncan, R.W. and Scott, S.L.: "Vertical Zero Net Liquid Flow: Effects of High Pressure on Holdup," paper presented at the BHR Group Multiphase 1998 Conference, Banff, Canada, Vol. 31, 43 – 60.

9. Reydon, R.F. and Gauvin, W.H.: "Theoretical and Experimental Studies of Confined Vortex Flow," *Cdn. J. of Chem. Eng.* (February 1981) **59**, 14.

10. Millington, B.C. and Thew, M.T.: "LDA of Component Velocities in Air-Water Models of Steam-Water Cyclone Separators," *Proc.,* 3rd International Conference on Multphase Flow, The Hague, The Netherlands (May 1987) 115-125.

11. Farchi, D.: ''A Study of Mixers and Separators for Two-Phase Flow in MHD Energy Conversion Systems,'' MS thesis, Ben Gurion U., Beersheba, Israel (1990).

12. Kurokawa, J. and Ohtaik, T.: ''Gas-Liquid Flow Characteristics and Gas-Separation Efficiency in a Cyclone Separator,'' *ASME FED Gas Liquid Flows,* (1995) **225**, 51-57.

13. Barbuceanu, N. and Scott, S.: "Novel Inlet Design Expands Range of Operability for Compact Separator," paper SPE 71555 presented at the 2001 SPE Annual Technical Conference and Exhibition, New Orleans, 30 September – 3 October.

14. Ivwo, I. and Scott, S.L.: "Expanding the Operational Envelope of Compact Cylindrical Cyclone Gas/Liquid Separators Using a Variable Inlet-Slot Configuration." MS thesis, Texas A&M U., College Station, Texas (2004).

15. Wolbert, D., Ma, B.F., Aurelle, Y. and Seureau, J.: "Efficiency Estimation of Liquid-Liquid Hydrocyclones Using Trajectory Analysis," *AIChe Journal* (June 1995) 1395.

16. Marti, S., Erdal, F., Shoham, O. , Shirazi, S. and Kouba, G.: "Analysis of Gas Carry-Under in Gas/Liquid Cylindrical Cyclones," paper presented at the Hydrocyclones 1996 International Meeting, Cambridge, England, 2-4 April.

17. Movafaghian, S.: ''The Effects of Geometry, Fluid Properties and Pressure on the Flow Hydrodynamics in CCGL Separators,'' MS thesis, U. of Tulsa, Tulsa, Oklahoma (1997).

18. Wang, S., Mohan, R., Shoham, O., Marrelli, J.D. and Kouba, G.E.: "Optimal Control Strategy and Experimental Investigation of Gas/Liquid Compact Separators," paper SPE 63120 presented at the 2000 SPE Annual Technical Conference and Exhibition, Dallas, 1-4 October.

19. Mantilla, I., Shirazi, S., and Shoham, O.: ''Flow Field Prediction and Bubble Trajectory Model in CCGL Separators,'' *ASME J. Energy Res. Tech.*(March 1999) **121**,

20. Gomez, L., Mohan, R., Shoham, O. and Kouba, G.: "Enhanced Mechanistic Model and Field Application Design of Gas-Liquid Cylindrical Cyclone Separator," paper SPE

49174 presented at the 1998 SPE Annual Technical Conference and Exhibition, New 27-30 Orleans, September.

21. Sagar, Neeraj S., Castanier, Louis M.: "Oil-Foam Interaction in a Micromodel" Prepared for U.S. Department of Energy, Assistant Secretary for Fossil Energy, Houston, November 1997.

22. Holm, L.W.; "The Mechanisms of Gas and Liquid Flow through Porous Media in the Presence of Foam," *SPEJ*, 359-369, December 1968.

23. Zhang, H.Q. and Sarica, C.: "Unified Modeling of Gas/Oil/Water Pipe Flow-Basic Approaches and preliminary Validation," paper SPE 95749 presented at the 2005 SPE Annual Technical Conference and Exhibition, Dallas, 9-12 October.

24. Kouba, G.E., Mohan, R., Shoham, O., Wang, S., Gomez, L. *et al.*: ''Oil-Water Separation in a Novel Liquid-Liquid Cylindrical Cyclone (LLCC) Compact separator-Experiments and Modeling,'' *J. of Fluid Engineering*, (July 2004) **126**, 553-564.

APPENDIX A

SAMPLE CALCULATIONS

Input parameters

ρ_w — water density, ρ_o — oil density

h_{osep} — oil volume fraction in CCGL separator

h_{wsep} — water volume fraction in CCGL separator

h_{otank} — oil volume fraction in mixing tank

h_{wtank} — water volume fraction in mixing tank

T —temperature, ^{o}F

$P_{in\text{-}situ}$ —pressure, psig

ZNLF holdup

Gas density, g/cc

$$\rho_g = \frac{29}{10.73}\frac{zT}{P_{in-situ}} \quad \text{(A.1)}$$

Liquid mixture density, g/cc

$$\rho_{lmix} = h_{osep}\rho_o + h_{wsep}\rho_w \quad \text{(A.2)}$$

Bubble rise velocity, ft/s

$$\upsilon_{Go} = C_o\upsilon_{SG} + 0.35\sqrt{gd_{sep}\left[\frac{\rho_{lmix} - \rho_g}{\rho_{lmix}}\right]} \quad \text{(A.3)}$$

Liquid mixture ZNLF holdup

$$H_{Lomix} = \left[\frac{\upsilon_{SG}}{(1 - H_{Lmix})}\right] * \left[1 - \frac{L_d}{L_{gi}}\right] \quad \text{(A.4)}$$

LCO operational envelope

Liquid mixture density, g/cc

$$\rho_{lmix} = h_{o\tan k}\rho_o + h_{w\tan k}\rho_w \quad \text{(A.5)}$$

Liquid mixture velocity, ft/s

$$V_{lmix} = \frac{Q_{lmix}}{A_{sep}} \quad \text{(A.6)}$$

Gas velocity at in-situ condition, ft/s 1

$$V_{sg} = \frac{Q_{Gin-situ}}{A_{sep}} \quad \text{(A.7)}$$

APPENDIX B

TEST DATA SET

Table B.1 ZNLF separator operations for slot #1 at (recombinations Nos1-3) (water)

Zero-net-liquid flow[water] [Slot (1)/Recombination (1)]								
Runs	Pressure (Psig)	Temp (oF)	Gas Rates Qg(ft3/min)	Qg(lb/min)	Gas Velocity (ft/sec)	hL (inches)	Bubble rise Vel (ft/sec)	ZNLF hold-up
1	2.187	72.488	1.191	0.102	0.404	40.000	1.416	0.814
2	1.710	72.482	2.220	0.185	0.754	31.350	1.818	0.459
3	1.611	72.493	3.213	0.266	1.091	26.750	2.206	0.338
4	1.320	72.452	5.586	0.454	1.896	17.750	3.132	0.175
5	1.542	72.043	8.090	0.667	2.746	12.250	4.109	0.142
6	1.602	71.755	13.587	1.126	4.613	8.000	6.256	0.093
7	1.688	71.416	19.977	1.665	6.782	5.000	8.750	0.068
8	2.170	70.847	33.125	2.845	11.245	0.000	13.883	0.000

Zero-net-liquid flow[water] [Slot (1)/Recombination (2)]								
Runs	Pressure (Psig)	Temp (oF)	Gas Rates Qg(ft3/min)	Qg(lb/min)	Gas Velocity (ft/sec)	hL (inches)	Bubble rise Vel (ft/sec)	ZNLF hold-up
1	2.935	71.108	0.900	0.081	0.306	40.000	1.302	0.765
2	2.822	71.147	1.554	0.139	0.528	37.750	1.558	0.624
3	1.985	71.593	2.743	0.233	0.931	29.750	2.022	0.401
4	1.673	71.736	4.220	0.351	1.433	23.500	2.599	0.264
5	1.776	71.681	5.817	0.487	1.975	16.500	3.222	0.160
6	1.735	71.766	9.144	0.764	3.104	11.600	4.521	0.091
7	1.729	71.431	13.182	1.101	4.475	8.000	6.097	0.053
8	2.221	71.635	19.701	1.695	6.688	4.250	8.642	0.024

Zero-net-liquid flow[water] [Slot (1)/Recombination (3)]								
Runs	Pressure (Psig)	Temp (oF)	Gas Rates Qg(ft3/min)	Qg(lb/min)	Gas Velocity (ft/sec)	hL (inches)	Bubble rise Vel (ft/sec)	ZNLF hold-up
1	2.803	71.803	0.955	0.085	0.324	40.000	1.324	0.755
2	1.838	71.821	2.324	0.195	0.789	31.750	1.858	0.457
3	1.657	71.908	3.955	0.329	1.343	23.250	2.495	0.268
4	1.552	71.902	5.527	0.456	1.876	19.250	3.109	0.191
5	1.642	71.785	8.885	0.738	3.016	11.250	4.420	0.089
6	1.544	71.566	13.650	1.127	4.634	7.250	6.280	0.048
7	1.711	71.144	20.855	1.742	7.080	4.500	9.093	0.025
8	2.163	70.763	31.925	2.741	10.838	0.000	13.415	0.000

Table B.2 ZNLF separator operations for slot #2 at (recombinations Nos1-3) (water)

Zero-net-liquid flow[water] [Slot (2)/Recombination (1)]								
Runs	Pressure (Psig)	Temp (oF)	Gas Rates Qg(ft3/min)	Qg(lb/min)	Gas Velocity (ft/sec)	hL (inches)	Bubble rise Vel (ft/sec)	ZNLF hold-up
1	2.467	71.173	1.169	0.102	0.397	40.000	1.407	0.718
2	1.729	71.160	2.212	0.185	0.751	32.750	1.815	0.480
3	1.628	71.141	3.202	0.266	1.087	24.250	2.201	0.341
4	1.489	71.150	5.515	0.454	1.872	19.350	3.104	0.192
5	1.521	71.136	8.086	0.667	2.745	12.500	4.108	0.124
6	1.632	71.146	13.547	1.126	4.599	8.250	6.240	0.054
7	1.635	71.156	20.033	1.665	6.801	4.750	8.772	0.027
8	2.124	71.184	33.237	2.845	11.284	0.000	13.927	0.000

Zero-net-liquid flow[water] [Slot (2)/Recombination (2)]								
Runs	Pressure (Psig)	Temp (oF)	Gas Rates Qg(ft3/min)	Qg(lb/min)	Gas Velocity (ft/sec)	hL (inches)	Bubble rise Vel (ft/sec)	ZNLF hold-up
1	2.933	71.351	0.000 0.641	0.058	0.218	40.000	1.201	0.819
2	2.822	71.338	1.555	0.139	0.528	38.250	1.558	0.632
3	1.985	71.360	2.742	0.233	0.931	31.500	2.021	0.425
4	1.684	71.361	4.215	0.351	1.431	25.750	2.596	0.289
5	1.760	71.368	5.819	0.487	1.976	20.250	3.223	0.196
6	1.738	71.360	9.135	0.764	3.101	13.000	4.517	0.102
7	1.567	71.350	13.311	1.101	4.519	8.000	6.148	0.053
8	2.388	71.321	19.496	1.695	6.619	4.250	8.563	0.024

Zero-net-liquid flow[water] [Slot (2)/Recombination (3)]								
Runs	Pressure (Psig)	Temp (oF)	Gas Rates Qg(ft3/min)	Qg(lb/min)	Gas Velocity (ft/sec)	hL (inches)	Bubble rise Vel (ft/sec)	ZNLF hold-up
1	2.795	71.256	0.954	0.085	0.324	40.000	1.323	0.755
2	1.933	71.268	2.308	0.195	0.784	31.750	1.852	0.458
3	1.689	71.277	3.942	0.329	1.338	22.350	2.490	0.258
4	1.469	71.280	5.549	0.456	1.884	19.850	3.117	0.196
5	1.638	71.299	8.879	0.738	3.014	12.550	4.417	0.100
6	1.544	71.284	13.643	1.127	4.632	7.450	6.277	0.049
7	1.752	71.283	20.808	1.742	7.064	4.600	9.075	0.025
8	2.493	71.275	31.342	2.741	10.640	0.000	13.187	0.000

Table B.3 ZNLF separator operations for slot #3 at (recombinations Nos1-3) (water)

Zero-net-liquid flow[water] [Slot (3)/Recombination (1)]								
Runs	Pressure (Psig)	Temp (oF)	Gas Rates Qg(ft3/min)	Qg(lb/min)	Gas Velocity (ft/sec)	hL (inches)	Bubble rise Vel (ft/sec)	ZNLF hold-up
1	2.147	71.374	1.191	0.102	0.404	40.000	1.416	0.714
2	1.688	71.378	2.218	0.185	0.753	31.650	1.817	0.463
3	1.634	71.374	3.202	0.266	1.087	23.250	2.201	0.329
4	1.445	71.369	5.532	0.454	1.878	19.250	3.111	0.219
5	1.483	71.392	8.109	0.667	2.753	12.350	4.117	0.132
6	1.636	71.362	13.549	1.126	4.600	8.950	6.241	0.059
7	1.600	71.337	20.082	1.665	6.817	4.550	8.791	0.026
8	2.433	71.315	32.646	2.845	11.083	0.000	13.696	0.000

Zero-net-liquid flow[water] [Slot (3)/Recombination (2)]								
Runs	Pressure (Psig)	Temp (oF)	Gas Rates Qg(ft3/min)	Qg(lb/min)	Gas Velocity (ft/sec)	hL (inches)	Bubble rise Vel (ft/sec)	ZNLF hold-up
1	2.830	71.372	0.909	0.081	0.309	40.000	1.306	0.764
2	2.887	71.383	1.549	0.139	0.526	37.250	1.556	0.616
3	2.030	71.377	2.734	0.233	0.928	30.500	2.018	0.412
4	1.712	71.374	4.208	0.351	1.428	25.250	2.594	0.284
5	1.817	71.375	5.799	0.487	1.969	21.250	3.215	0.206
6	1.775	71.363	9.115	0.764	3.094	13.150	4.509	0.103
7	1.769	71.342	13.148	1.101	4.464	8.950	6.084	0.060
8	2.272	71.323	19.630	1.695	6.664	4.500	8.615	0.025

Zero-net-liquid flow[water] [Slot (3)/Recombination (3)]								
Runs	Pressure (Psig)	Temp (oF)	Gas Rates Qg(ft3/min)	Qg(lb/min)	Gas Velocity (ft/sec)	hL (inches)	Bubble rise Vel (ft/sec)	ZNLF hold-up
1	2.868	71.547	0.951	0.085	0.323	40.000	1.322	0.756
2	1.880	71.821	2.318	0.195	0.787	32.750	1.856	0.472
3	1.695	71.908	3.945	0.329	1.339	21.450	2.491	0.248
4	1.587	71.902	5.515	0.456	1.872	19.250	3.104	0.191
5	1.680	71.785	8.864	0.738	3.009	12.750	4.412	0.101
6	1.579	71.566	13.621	1.127	4.624	7.750	6.269	0.051
7	1.750	71.144	20.805	1.742	7.063	4.800	9.073	0.027
8	2.213	70.763	31.831	2.741	10.806	0.000	13.378	0.000

Table B.4 ZNLF separator operations for slot #1 at (recombinations Nos1-3) (oil)

Zero-net-liquid flow[Oil] [Slot (1)/Recombination (1)]								
Runs	Pressure (Psig)	Temp (oF)	Gas Rates Qg(ft3/min)	Qg(lb/min)	Gas Velocity (ft/sec)	hL (inches)	Bubble rise Vel (ft/sec)	ZNLF hold-up
1	2.994	75.666	0.918	0.082	0.312	32.000	1.309	0.670
2	2.339	75.735	1.630	0.140	0.553	27.350	1.587	0.485
3	2.104	75.323	2.773	0.235	0.941	22.650	2.033	0.304
4	1.918	75.810	4.236	0.355	1.438	19.150	2.605	0.214
5	1.999	75.906	5.849	0.493	1.986	14.900	3.234	0.144
6	1.965	75.977	9.190	0.772	3.120	10.250	4.539	0.080
7	2.023	75.721	13.200	1.114	4.481	6.250	6.104	0.042
8	1.618	75.161	21.087	1.738	7.159	0.000	9.184	0.000

Zero-net-liquid flow[Oil] [Slot (1)/Recombination (2)]								
Runs	Pressure (Psig)	Temp (oF)	Gas Rates Qg(ft3/min)	Qg(lb/min)	Gas Velocity (ft/sec)	hL (inches)	Bubble rise Vel (ft/sec)	ZNLF hold-up
1	2.961	74.842	0.908	0.081	0.308	31.750	1.305	0.606
2	2.313	74.909	1.612	0.139	0.547	27.850	1.580	0.455
3	2.081	74.500	2.742	0.233	0.931	23.250	2.021	0.314
4	1.897	74.982	4.189	0.351	1.422	18.950	2.586	0.213
5	1.978	75.076	5.783	0.487	1.963	14.850	3.209	0.144
6	1.943	75.146	9.087	0.764	3.085	10.500	4.498	0.082
7	2.000	74.892	13.053	1.101	4.431	6.750	6.047	0.045
8	1.600	74.337	20.847	1.719	7.077	0.000	9.090	0.000

Zero-net-liquid flow[Oil] [Slot (1)/Recombination (3)]								
Runs	Pressure (Psig)	Temp (oF)	Gas Rates Qg(ft3/min)	Qg(lb/min)	Gas Velocity (ft/sec)	hL (inches)	Bubble rise Vel (ft/sec)	ZNLF hold-up
1	2.961	74.827	0.908	0.081	0.308	32.350	1.305	0.618
2	2.313	74.895	1.612	0.139	0.547	26.450	1.580	0.432
3	2.081	74.486	2.742	0.233	0.931	22.950	2.021	0.310
4	1.897	74.968	4.188	0.351	1.422	18.750	2.586	0.211
5	1.977	75.062	5.782	0.487	1.963	15.000	3.208	0.146
6	1.943	75.132	9.085	0.764	3.084	9.800	4.498	0.097
7	2.000	74.878	13.050	1.101	4.430	6.550	6.046	0.054
8	1.600	74.323	20.843	1.718	7.076	0.000	9.088	0.000

Table B.5 ZNLF separator operations for slot #2 at (recombinations Nos1-3) (oil)

Zero-net-liquid flow[Oil] [Slot (2)/Recombination (1)]								
Runs	Pressure (Psig)	Temp (oF)	Gas Rates Qg(ft3/min)	Qg(lb/min)	Gas Velocity (ft/sec)	hL (inches)	Bubble rise Vel (ft/sec)	ZNLF hold-up
1	2.994	75.674	0.918	0.082	0.312	32.000	1.309	0.660
2	2.339	75.750	1.630	0.140	0.553	27.350	1.587	0.465
3	2.105	75.345	2.774	0.235	0.942	22.650	2.034	0.334
4	1.919	75.841	4.238	0.355	1.439	19.150	2.606	0.234
5	2.000	75.944	5.852	0.493	1.987	14.900	3.236	0.154
6	1.966	76.023	9.195	0.773	3.122	10.250	4.541	0.082
7	2.024	75.774	13.210	1.114	4.484	6.250	6.108	0.045
8	1.619	75.222	21.105	1.739	7.165	0.000	9.190	0.000

Zero-net-liquid flow[Oil] [Slot (2)/Recombination (2)]								
Runs	Pressure (Psig)	Temp (oF)	Gas Rates Qg(ft3/min)	Qg(lb/min)	Gas Velocity (ft/sec)	hL (inches)	Bubble rise Vel (ft/sec)	ZNLF hold-up
1	2.961	74.842	0.908	0.081	0.308	31.750	1.305	0.606
2	2.313	74.909	1.612	0.139	0.547	27.850	1.580	0.455
3	2.081	74.500	2.742	0.233	0.931	23.250	2.021	0.314
4	1.897	74.982	4.189	0.351	1.422	18.950	2.586	0.213
5	1.978	75.076	5.783	0.487	1.963	14.850	3.209	0.144
6	1.943	75.146	9.087	0.764	3.085	10.500	4.498	0.082
7	2.000	74.892	13.053	1.101	4.431	6.750	6.047	0.045
8	1.600	74.337	20.847	1.719	7.077	0.000	9.090	0.000

Zero-net-liquid flow[Oil] [Slot (2)/Recombination (3)]								
Runs	Pressure (Psig)	Temp (oF)	Gas Rates Qg(ft3/min)	Qg(lb/min)	Gas Velocity (ft/sec)	hL (inches)	Bubble rise Vel (ft/sec)	ZNLF hold-up
1	2.961	74.835	0.908	0.081	0.308	32.350	1.305	0.618
2	2.313	74.910	1.612	0.139	0.547	26.450	1.580	0.432
3	2.082	74.508	2.742	0.233	0.931	22.950	2.021	0.310
4	1.898	74.998	4.188	0.351	1.422	18.750	2.586	0.211
5	1.978	75.099	5.782	0.487	1.963	15.000	3.208	0.146
6	1.944	75.177	9.085	0.764	3.084	9.800	4.498	0.077
7	2.001	74.930	13.050	1.101	4.430	6.550	6.046	0.044
8	1.601	74.383	20.843	1.718	7.076	0.000	9.088	0.000

Table B.6 ZNLF separator operations for slot #3 at (recombinations Nos1-3) (oil)

Zero-net-liquid flow[Oil] [Slot (3)/Recombination (1)]								
Runs	Pressure (Psig)	Temp (oF)	Gas Rates Qg(ft3/min)	Qg(lb/min)	Gas Velocity (ft/sec)	hL (inches)	Bubble rise Vel (ft/sec)	ZNLF hold-up
1	3.001	75.848	0.920	0.082	0.312	32.000	1.310	0.651
2	2.344	75.894	1.633	0.140	0.555	27.350	1.589	0.495
3	2.108	75.458	2.778	0.236	0.943	22.650	2.035	0.325
4	1.921	75.924	4.243	0.356	1.440	19.150	2.607	0.214
5	2.002	75.997	5.856	0.493	1.988	14.900	3.237	0.164
6	1.966	76.046	9.198	0.773	3.123	10.250	4.542	0.091
7	2.024	75.767	13.208	1.114	4.484	6.250	6.108	0.055
8	1.619	75.184	21.094	1.738	7.161	0.000	9.186	0.000

Zero-net-liquid flow[Oil] [Slot (3)/Recombination (2)]								
Runs	Pressure (Psig)	Temp (oF)	Gas Rates Qg(ft3/min)	Qg(lb/min)	Gas Velocity (ft/sec)	hL (inches)	Bubble rise Vel (ft/sec)	ZNLF hold-up
1	2.966	74.961	0.909	0.081	0.309	31.750	1.306	0.606
2	2.316	75.014	1.614	0.139	0.548	27.850	1.581	0.455
3	2.084	74.589	2.745	0.233	0.932	23.250	2.023	0.313
4	1.899	75.057	4.193	0.352	1.424	18.950	2.588	0.213
5	1.979	75.136	5.788	0.488	1.965	14.850	3.211	0.144
6	1.944	75.191	9.092	0.764	3.087	10.500	4.501	0.082
7	2.001	74.921	13.058	1.102	4.433	6.750	6.049	0.045
8	1.601	74.352	20.851	1.719	7.079	0.000	9.091	0.000

Zero-net-liquid flow[Oil] [Slot (3)/Recombination (3)]								
Runs	Pressure (Psig)	Temp (oF)	Gas Rates Qg(ft3/min)	Qg(lb/min)	Gas Velocity (ft/sec)	hL (inches)	Bubble rise Vel (ft/sec)	ZNLF hold-up
1	2.963	74.887	0.908	0.081	0.308	32.350	1.306	0.618
2	2.314	74.947	1.613	0.139	0.548	26.450	1.581	0.432
3	2.082	74.531	2.743	0.233	0.931	22.950	2.022	0.309
4	1.898	75.005	4.190	0.351	1.423	18.750	2.587	0.211
5	1.978	75.092	5.785	0.487	1.964	15.000	3.209	0.146
6	1.943	75.154	9.088	0.764	3.085	9.800	4.499	0.077
7	2.000	74.893	13.053	1.101	4.431	6.550	6.047	0.044
8	1.600	74.331	20.845	1.719	7.077	0.000	9.089	0.000

Table B.7 LCO separator operations at slot #1(recombination#1) (water)

Liquid Carry-Over(LCO)[Water] 3-psig [Slot (1)/Recombination (1)]								
Runs	Pressure (Psig)	Temp (oF)	Rates Ql(lb/min)	Qg(lb/min)	Qg(ft3/min)	Liq Density g/cc	Liq Vel (ft/sec)	Gas Vel (ft/sec)
1	3.389	71.859	153.671	0.541	5.886	0.996	0.827	1.998
2	3.358	71.857	135.492	0.882	9.614	0.994	0.731	3.264
3	2.874	71.871	126.958	1.274	14.266	0.995	0.684	4.843
4	2.893	71.815	110.855	1.796	20.084	0.995	0.597	6.818
5	2.878	71.516	97.288	2.387	26.705	0.994	0.525	9.066
6	2.824	71.263	89.326	3.322	37.265	0.994	0.482	12.651
7	3.286	70.709	72.980	3.808	41.579	0.995	0.393	14.116

Liquid Carry-Over(LCO)[Water] 6-psig [Slot (1)/Recombination (1)]								
Runs	Pressure (Psig)	Temp (oF)	Rates Ql(lb/min)	Qg(lb/min)	Qg(ft3/min)	Liq Density g/cc	Liq Vel (ft/sec)	Gas Vel (ft/sec)
1	6.720	71.931	200.559	0.650	5.970	0.996	1.080	2.027
2	5.754	72.000	182.841	1.060	10.205	0.994	0.986	3.465
3	5.795	72.087	176.641	1.533	14.722	0.995	0.952	4.998
4	5.767	72.103	164.389	2.162	20.797	0.995	0.886	7.060
5	5.663	71.873	152.747	2.876	27.797	0.994	0.824	9.437
6	6.592	71.690	141.547	4.007	37.019	0.994	0.763	12.568
7	6.422	71.204	130.326	4.597	42.774	0.995	0.702	14.521

Liquid Carry-Over(LCO)[Water] 10-psig [Slot (1)/Recombination (1)]								
Runs	Pressure (Psig)	Temp (oF)	Rates Ql(lb/min)	Qg(lb/min)	Qg(ft3/min)	Liq Density g/cc	Liq Vel (ft/sec)	Gas Vel (ft/sec)
1	9.745	72.003	301.039	0.651	5.243	0.996	1.620	1.780
2	8.344	72.144	274.628	1.065	9.097	0.994	1.481	3.088
3	8.404	72.303	265.491	1.542	13.143	0.995	1.431	4.462
4	8.365	72.391	247.241	2.179	18.613	0.995	1.332	6.319
5	8.214	72.232	229.884	2.905	24.966	0.994	1.240	8.476
6	9.562	72.120	213.170	4.055	32.904	0.994	1.149	11.170
7	9.317	71.702	196.401	4.661	38.181	0.995	1.059	12.962

Table B.8 LCO separator operations at slot #2 (recombination#1) (water)

Liquid Carry-Over(LCO)[Water] 3-psig [Slot (2)/Recombination (1)]								
Runs	Pressure (Psig)	Temp (oF)	Rates Ql(lb/min)	Qg(lb/min)	Qg(ft3/min)	Liq Density g/cc	Liq Vel (ft/sec)	Gas Vel (ft/sec)
1	3.424	72.585	155.223	0.546	5.942	0.996	0.836	2.017
2	3.393	72.589	136.874	0.891	9.707	0.994	0.738	3.295
3	2.904	72.612	128.266	1.287	14.409	0.995	0.692	4.892
4	2.923	72.562	112.008	1.814	20.287	0.995	0.603	6.887
5	2.908	72.266	98.309	2.412	26.977	0.994	0.530	9.158
6	2.854	72.018	90.273	3.357	37.649	0.994	0.487	12.781
7	3.321	71.465	73.761	3.849	42.002	0.995	0.398	14.259

Liquid Carry-Over(LCO)[Water] 6-psig [Slot (2)/Recombination (1)]								
Runs	Pressure (Psig)	Temp (oF)	Rates Ql(lb/min)	Qg(lb/min)	Qg(ft3/min)	Liq Density g/cc	Liq Vel (ft/sec)	Gas Vel (ft/sec)
1	6.788	72.658	202.585	0.656	6.020	0.996	1.090	2.044
2	5.812	72.735	184.706	1.071	10.294	0.994	0.996	3.495
3	5.854	72.830	178.460	1.548	14.851	0.995	0.962	5.042
4	5.827	72.852	166.099	2.185	20.982	0.995	0.895	7.123
5	5.722	72.628	154.351	2.906	28.046	0.994	0.832	9.521
6	6.662	72.450	143.048	4.049	37.343	0.994	0.771	12.677
7	6.491	71.966	131.721	4.646	43.153	0.995	0.710	14.650

Liquid Carry-Over(LCO)[Water] 10-psig [Slot (2)/Recombination (1)]								
Runs	Pressure (Psig)	Temp (oF)	Rates Ql(lb/min)	Qg(lb/min)	Qg(ft3/min)	Liq Density g/cc	Liq Vel (ft/sec)	Gas Vel (ft/sec)
1	9.843	72.730	304.079	0.658	5.282	0.996	1.637	1.793
2	8.429	72.880	277.429	1.076	9.168	0.994	1.496	3.113
3	8.491	73.048	268.225	1.558	13.248	0.995	1.446	4.497
4	8.452	73.144	249.812	2.202	18.762	0.995	1.346	6.369
5	8.300	72.991	232.298	2.935	25.169	0.994	1.253	8.545
6	9.663	72.885	215.430	4.098	33.162	0.994	1.162	11.258
7	9.416	72.469	198.503	4.711	38.486	0.995	1.070	13.065

Table B.9 LCO separator operations at slot #3 (recombination#1) (water)

Liquid Carry-Over(LCO)[Water] 3-psig [Slot (3)/Recombination (1)]								
Runs	Pressure (Psig)	Temp (oF)	Rates Ql(lb/min)	Qg(lb/min)	Qg(ft3/min)	Liq Density g/cc	Liq Vel (ft/sec)	Gas Vel (ft/sec)
1	3.424	72.599	155.254	0.547	5.943	0.996	0.836	2.018
2	3.394	72.618	136.928	0.892	9.710	0.994	0.738	3.297
3	2.905	72.655	128.342	1.288	14.417	0.995	0.692	4.894
4	2.925	72.620	112.096	1.816	20.303	0.995	0.604	6.892
5	2.911	72.338	98.407	2.414	27.003	0.994	0.531	9.167
6	2.858	72.103	90.380	3.361	37.692	0.994	0.487	12.796
7	3.326	71.564	73.863	3.855	42.057	0.995	0.398	14.278

Liquid Carry-Over(LCO)[Water] 6-psig [Slot (3)/Recombination (1)]								
Runs	Pressure (Psig)	Temp (oF)	Rates Ql(lb/min)	Qg(lb/min)	Qg(ft3/min)	Liq Density g/cc	Liq Vel (ft/sec)	Gas Vel (ft/sec)
1	6.789	72.672	202.625	0.656	6.021	0.996	1.091	2.044
2	5.815	72.763	184.780	1.072	10.297	0.994	0.996	3.496
3	5.858	72.873	178.566	1.549	14.859	0.995	0.963	5.044
4	5.832	72.910	166.230	2.186	20.996	0.995	0.896	7.128
5	5.728	72.700	154.504	2.909	28.070	0.994	0.833	9.529
6	6.669	72.536	143.218	4.054	37.379	0.994	0.772	12.690
7	6.500	72.065	131.903	4.652	43.203	0.995	0.711	14.667

Liquid Carry-Over(LCO)[Water] 10-psig [Slot (3)/Recombination (1)]								
Runs	Pressure (Psig)	Temp (oF)	Rates Ql(lb/min)	Qg(lb/min)	Qg(ft3/min)	Liq Density g/cc	Liq Vel (ft/sec)	Gas Vel (ft/sec)
1	9.845	72.745	304.140	0.658	5.282	0.996	1.637	1.793
2	8.433	72.909	277.539	1.076	9.171	0.994	1.497	3.113
3	8.496	73.091	268.385	1.559	13.254	0.995	1.447	4.499
4	8.458	73.202	250.010	2.204	18.774	0.995	1.347	6.373
5	8.309	73.063	232.528	2.938	25.188	0.994	1.254	8.551
6	9.675	72.971	215.686	4.103	33.191	0.994	1.163	11.268
7	9.429	72.570	198.778	4.718	38.526	0.995	1.071	13.079

Table B.10 LCO separator operations at slot #1(recombination#1) (oil)

Liquid Carry-Over(LCO)[Oil] [Slot (1)/Recombination (1)] 3-psig								
Runs	Pressure (Psig)	Temp (oF)	Rates Ql(lb/min)	Qg(lb/min)	Qg(ft3/min)	Liq Density g/cc	Liq Vel (ft/sec)	Gas Vel (ft/sec)
1	3.671	72.599	137.080	0.410	4.397	0.764	0.962	1.493
2	3.080	71.836	123.054	0.534	5.915	0.764	0.864	2.008
3	3.019	71.841	97.475	0.886	9.840	0.764	0.684	3.341
4	3.069	71.813	67.449	1.299	14.384	0.764	0.474	4.883
5	3.072	71.815	34.482	1.856	20.547	0.764	0.242	6.975
6	3.053	71.821	26.937	2.498	27.683	0.764	0.189	9.398
7	3.236	71.564	19.753	3.154	34.582	0.764	0.139	11.740

Liquid Carry-Over(LCO)[Oil] [Slot (1)/Recombination (1)] 6-psig								
Runs	Pressure (Psig)	Temp (oF)	Rates Ql(lb/min)	Qg(lb/min)	Qg(ft3/min)	Liq Density g/cc	Liq Vel (ft/sec)	Gas Vel (ft/sec)
1	6.052	73.895	179.688	0.492	4.687	0.764	1.262	1.591
2	6.064	74.051	166.373	0.562	5.348	0.764	1.168	1.816
3	6.077	74.208	138.895	0.875	8.326	0.764	0.975	2.826
4	6.090	74.366	104.274	1.270	12.075	0.764	0.732	4.099
5	6.103	74.523	58.351	1.853	17.621	0.764	0.410	5.982
6	6.116	74.681	53.050	2.467	23.449	0.764	0.372	7.961
7	6.208	74.199	38.351	3.228	30.512	0.764	0.269	10.358

Liquid Carry-Over(LCO)[Oil] [Slot (1)/Recombination (1)] 10-psig								
Runs	Pressure (Psig)	Temp (oF)	Rates Ql(lb/min)	Qg(lb/min)	Qg(ft3/min)	Liq Density g/cc	Liq Vel (ft/sec)	Gas Vel (ft/sec)
1	9.845	74.629	263.298	0.519	4.181	0.764	1.849	1.419
2	9.866	74.788	243.117	0.589	4.746	0.764	1.707	1.611
3	9.887	74.946	212.061	0.831	6.686	0.764	1.489	2.270
4	9.908	75.105	151.825	1.299	10.450	0.764	1.066	3.548
5	9.929	75.264	80.182	1.856	14.923	0.764	0.563	5.066
6	9.950	75.424	67.947	2.498	20.073	0.764	0.477	6.814
7	10.942	74.410	49.418	3.330	25.676	0.764	0.347	8.717

Table B.11 ZNLF operation for a range of water cut

Zero-net-liquid flow[Oil/Water] [Slot (1)/Recombination (1)]							Water cut 90%			
Runs	Gas Rates Qg(ft3/min)	Qg(lb/min)	Gas Velocity (ft/sec)	hL (inches)	hL(Oil) (inches)	hL(Water) (inches)	Gas density (g/cc)	Mixture density (g/cc)	Bubble rise Vel (ft/sec)	ZNLF hold-up
1	0.507721	0.044448	0.17236443	40	7.944	32.056	0.08754464	0.951479936	1.143768866	0.849301348
2	0.671191	0.057755	0.22786026	36.15	6.059	30.091	0.08604892	0.958739691	1.208763417	0.733386881
3	1.544832	0.129264	0.5244497	29	4.27905	24.72095	0.08367538	0.96343708	1.551348815	0.479906164
4	2.247708	0.18464	0.76306664	22.0625	2.4883	19.5742	0.08214609	0.971581444	1.826952798	0.321190405
5	3.055723	0.253537	1.03737671	15.4375	1.0385	14.399	0.0829712	0.982242381	2.142449631	0.199066095
6	3.429923	0.284763	1.16441251	10.7	0.7224	9.9776	0.08302308	0.982185516	2.288510879	0.131393875
7	5.309216	0.460754	1.80240731	7.25	0.4044	6.8456	0.08678386	0.984934254	3.020345421	0.073088092

Zero-net-liquid flow[Oil/Water] [Slot (1)/Recombination (1)]							Water cut 80%			
Runs	Gas Rates Qg(ft3/min)	Qg(lb/min)	Gas Velocity (ft/sec)	hL (inches)	hL(Oil) (inches)	hL(Water) (inches)	Gas density (g/cc)	Mixture density (g/cc)	Bubble rise Vel (ft/sec)	ZNLF hold-up
1	0.47469	0.04227	0.16115091	40	15.84	24.16	0.08904704	0.90524096	1.127556274	0.857079499
2	0.907463	0.078665	0.3080716	33.65	12.06873	21.58128	0.08668697	0.913988762	1.298354429	0.641639459
3	1.630496	0.137039	0.55353146	24.85	8.51441	16.33559	0.08404751	0.917741835	1.582333856	0.403924548
4	1.848991	0.153421	0.62770768	19.9375	4.946055	14.99145	0.08297549	0.939890211	1.669352107	0.311015657
5	3.315469	0.276766	1.12555697	13.5625	2.06212	11.50038	0.08347703	0.962384812	2.242679875	0.168893693
6	4.155868	0.345361	1.41086105	8.775	1.432975	7.342025	0.08310208	0.959748141	2.570858677	0.098984235
7	5.72137	0.503993	1.94232819	5.65	0.80136	4.84864	0.08808951	0.964776891	3.179593346	0.054964168

Zero-net-liquid flow[Oil/Water] [Slot (1)/Recombination (1)]							Water cut 70%			
Runs	Gas Rates Qg(ft3/min)	Qg(lb/min)	Gas Velocity (ft/sec)	hL (inches)	hL(Oil) (inches)	hL(Water) (inches)	Gas density (g/cc)	Mixture density (g/cc)	Bubble rise Vel (ft/sec)	ZNLF hold-up
1	0.534067	0.046577	0.18130859	40	24	16	0.08721095	0.857456	1.148990456	0.842201834
2	0.864296	0.072211	0.29341674	34.55	18.25	16.3	0.08354838	0.874269754	1.281126342	0.665925088
3	1.35636	0.112352	0.4604659	28.25	12.85	15.4	0.08283368	0.891451894	1.474611072	0.485714534
4	2.368828	0.19384	0.8041852	20.625	7.45	13.175	0.08182948	0.913389673	1.87162204	0.29407493
5	2.77242	0.229075	0.94119932	14.375	3.1	11.275	0.08262636	0.947485635	2.030426527	0.192787586
6	3.746137	0.314933	1.27176298	9.8	2.15	7.65	0.08406861	0.946610612	2.409741301	0.115699012
7	5.621965	0.496208	1.90858131	6.5	1.2	5.3	0.08826229	0.954755692	3.140191246	0.063733894

Table B.11 (continued)

Zero-net-liquid flow[Oil/Water] [Slot (1)/Recombination (1)]							Water cut 60%			
Runs	Gas Rates Qg(ft3/min)	Qg(lb/min)	Gas Velocity (ft/sec)	hL (inches)	hL(Oil) (inches)	hL(Water) (inches)	Gas density (g/cc)	Mixture density (g/cc)	Bubble rise Vel (ft/sec)	ZNLF hold-up
1	0.40801	0.03527	0.13851386	40	26.88	13.12	0.08644337	0.84059072	1.099186107	0.873985067
2	0.823325	0.068665	0.27950791	33.15	20.45825	12.69175	0.08339988	0.85344071	1.264004511	0.645489435
3	1.292582	0.107039	0.43881417	25.75	14.4177	11.3323	0.08281033	0.866846522	1.448350639	0.448709783
4	1.881038	0.153421	0.63858719	19.9375	8.36635	11.57115	0.08156185	0.89970614	1.68063033	0.309046771
5	2.748043	0.226766	0.93292373	12.8125	3.4844	9.3281	0.08251889	0.934297689	2.020329922	0.172402433
6	4.078772	0.345361	1.38468809	8.525	2.41875	6.10625	0.08467285	0.931540411	2.538520633	0.096871602
7	5.679107	0.503993	1.92798021	5.5	1.3512	4.1488	0.08874508	0.94045362	3.16149991	0.053648257

Zero-net-liquid flow[Oil/Water] [Slot (1)/Recombination (1)]							Water cut 50%			
Runs	Gas Rates Qg(ft3/min)	Qg(lb/min)	Gas Velocity (ft/sec)	hL (inches)	hL(Oil) (inches)	hL(Water) (inches)	Gas density (g/cc)	Mixture density (g/cc)	Bubble rise Vel (ft/sec)	ZNLF hold-up
1	0.448041	0.038705	0.15210383	40	28.8	11.2	0.08638666	0.8293472	1.114119843	0.863476244
2	0.800291	0.066666	0.27168793	33.65	22.0825	11.5675	0.08330191	0.844282175	1.25451831	0.65906257
3	1.152778	0.09544	0.39135276	26.25	15.677	10.573	0.0827914	0.85810741	1.393273834	0.471917789
4	1.873113	0.153039	0.63589679	19.9875	9.1635	10.824	0.08170326	0.890609969	1.67697185	0.31020926
5	2.606244	0.214613	0.88478466	13.4375	3.844	9.5935	0.08234571	0.930992107	1.964903696	0.184666805
6	4.093784	0.345102	1.38978453	9.025	2.6875	6.3375	0.08429909	0.928247091	2.544423247	0.102386803
7	5.614257	0.491661	1.9059647	5.625	1.512	4.113	0.08757361	0.935036288	3.136550155	0.055172426

Zero-net-liquid flow[Oil/Water] [Slot (1)/Recombination (1)]							Water cut 40%			
Runs	Gas Rates Qg(ft3/min)	Qg(lb/min)	Gas Velocity (ft/sec)	hL (inches)	hL(Oil) (inches)	hL(Water) (inches)	Gas density (g/cc)	Mixture density (g/cc)	Bubble rise Vel (ft/sec)	ZNLF hold-up
1	0.438436	0.038705	0.1488432	40	30.72	9.28	0.08827908	0.81810368	1.108405078	0.865714073
2	0.657962	0.056666	0.22336917	38.25	23.37825	14.87175	0.08612316	0.854833431	1.197862787	0.777935114
3	0.900882	0.07544	0.30583728	31.5	16.4737	15.0263	0.08374032	0.875498429	1.295365556	0.601570356
4	1.005001	0.083039	0.34118429	25.75	9.55835	16.19165	0.08262627	0.911050567	1.338596435	0.479669639
5	1.865079	0.154613	0.6331692	20.25	3.9804	16.2696	0.0828989	0.951957092	1.676255938	0.315025079
6	2.948745	0.245102	1.00105917	13	2.76275	10.23725	0.08312087	0.948219495	2.099029549	0.170002549
7	4.46212	0.391661	1.51482969	8	1.5432	6.4568	0.08777459	0.952815104	2.687545397	0.087270392

Zero-net-liquid flow[Oil/Water] [Slot (1)/Recombination (1)]							Water cut 30%			
Runs	Gas Rates Qg(ft3/min)	Qg(lb/min)	Gas Velocity (ft/sec)	hL (inches)	hL(Oil) (inches)	hL(Water) (inches)	Gas density (g/cc)	Mixture density (g/cc)	Bubble rise Vel (ft/sec)	ZNLF hold-up
1	0.283527	0.02527	0.09625375	40	32.64	7.36	0.08912629	0.80686016	1.046584796	0.908030623
2	0.561574	0.048665	0.19064695	31.75	24.83825	6.91175	0.08665859	0.814752388	1.157290674	0.662991131
3	1.037418	0.087039	0.35218939	22.35	17.5017	4.8483	0.08389979	0.814572787	1.344828063	0.412422135
4	1.615749	0.133421	0.54852503	19.85	10.15435	9.69565	0.08257531	0.878173554	1.575300248	0.323454023
5	2.484741	0.206766	0.8435362	12.55	4.2284	8.3216	0.0832141	0.919078851	1.916380543	0.175646175
6	3.690882	0.315361	1.25300472	7.45	2.93475	4.51525	0.08544333	0.905726733	2.38529236	0.088412044
7	4.586014	0.403993	1.55689004	4.6	1.6392	2.9608	0.08809235	0.914529085	2.733723145	0.04950604

Table B.11 (continued)

Zero-net-liquid flow[Oil/Water] [Slot (1)/Recombination (1)]							Water cut	20%		
Runs	Gas Rates Qg(ft3/min)	Qg(lb/min)	Gas Velocity (ft/sec)	hL (inches)	hL(Oil) (inches)	hL(Water) (inches)	Gas density (g/cc)	Mixture density (g/cc)	Bubble rise Vel (ft/sec)	ZNLF hold-up
1	0.21469	0.018705	0.0728843	40	34.56	5.44	0.08712454	0.79561664	1.020212149	0.928559667
2	0.557072	0.046666	0.18911835	33.1	26.30281	6.797188	0.08376973	0.811861909	1.157200115	0.692263726
3	0.667856	0.05544	0.22672822	25.75	18.53613	7.213875	0.08301208	0.82938245	1.202070658	0.522329276
4	1.134755	0.093039	0.38523415	19.9375	10.728	9.2095	0.08199078	0.871959788	1.387515887	0.360049788
5	1.87407	0.154613	0.63622166	13.3625	4.475625	8.886875	0.08250117	0.919543843	1.678395908	0.207430996
6	2.911743	0.245102	0.98849736	9.375	3.10675	6.26825	0.08417717	0.920375987	2.082607747	0.123130302
7	4.327886	0.381661	1.46925909	5.525	1.728	3.797	0.08818641	0.924739055	2.633449411	0.061062038

Zero-net-liquid flow[Oil/Water] [Slot (1)/Recombination (1)]							Water cut	10%		
Runs	Gas Rates Qg(ft3/min)	Qg(lb/min)	Gas Velocity (ft/sec)	hL (inches)	hL(Oil) (inches)	hL(Water) (inches)	Gas density (g/cc)	Mixture density (g/cc)	Bubble rise Vel (ft/sec)	ZNLF hold-up
1	0.185111	0.016449	0.06284267	40	36.48	3.52	0.08886198	0.78437312	1.006672228	0.937573853
2	0.434868	0.037755	0.14763172	35.9	27.76008	8.139925	0.08682009	0.81687131	1.107864192	0.777900985
3	0.58634	0.049264	0.19905442	29.375	19.56027	9.81473	0.08402028	0.84202391	1.170405453	0.609477609
4	0.90298	0.07464	0.30654968	22.9375	11.324	11.6135	0.08266008	0.882358201	1.29721096	0.437925937
5	1.242039	0.103537	0.42165565	17.8125	4.72223	13.09027	0.08336048	0.935901184	1.431982913	0.31418766
6	2.225678	0.184763	0.75558763	11.475	3.27746	8.19754	0.08301415	0.931096973	1.815959139	0.167511521
7	3.557504	0.300754	1.20772484	7.725	1.824	5.901	0.08454079	0.94269207	2.3356451	0.093263142

Table B.12 LCO separator performance operation for a range of water cut at different constant separator pressures.

			Liquid Carry-Over(LCO)[Oil/Water] [Slot (1)/Recombination (1)]			3-psig		Water cut	90%	
Runs	Pressure (Psig)	Temp (oF)	Rates Ql(lb/min)	Qg(lb/min)	Qg(ft3/min)	Water Density g/cc	Oil Density g/cc	Mix Density g/cc	Liq Vel (ft/sec)	Gas Vel (ft/sec)
0	3.424711	72.43618	200.1257	0	0	0.998233	0.76376	0.9747857	1.100892	0
1	3.380761	72.4585	148.7515	0.5307374	5.782963773	0.998233	0.76376	0.9747857	0.818282	1.963238
2	3.375587	72.37381	136.4512	0.85590547	9.327210854	0.998233	0.76376	0.9747857	0.750619	3.166462
3	2.888794	72.49626	124.4917	1.24925216	13.99369269	0.998233	0.76376	0.9747857	0.68483	4.75067
4	2.90811	72.48711	115.5091	1.75771653	19.66739842	0.998233	0.76376	0.9747857	0.635416	6.676817
5	2.892916	72.41386	95.55295	2.34433872	26.25025939	0.998233	0.76376	0.9747857	0.525637	8.911609
6	2.839371	72.38411	85.86121	3.19336012	35.8641616	0.998233	0.76376	0.9747857	0.472323	12.1754
7	3.30356	72.46079	73.78936	3.85069854	42.13766658	0.998233	0.76376	0.9747857	0.405916	14.30517

			Liquid Carry-Over(LCO)[Oil/Water] [Slot (1)/Recombination (1)]			6-psig		Water cut	90%	
Runs	Pressure (Psig)	Temp (oF)	Rates Ql(lb/min)	Qg(lb/min)	Qg(ft3/min)	Water Density g/cc	Oil Density g/cc	Mix Density g/cc	Liq Vel (ft/sec)	Gas Vel (ft/sec)
0	7.044619	72.47738	245.1257	0	0	0.998233	0.76376	0.9747857	1.348438	0
1	6.954214	72.45049	196.7485	0.63741562	5.799108427	0.998233	0.76376	0.9747857	1.056892	1.968719
2	5.783078	72.48138	177.3884	1.02879837	9.895578831	0.998233	0.76376	0.9747857	0.952894	3.359416
3	5.824654	72.37381	173.2091	1.50285035	14.42308915	0.998233	0.76376	0.9747857	0.930443	4.896444
4	6.197116	72.36351	160.9108	2.1162907	19.94798203	0.998233	0.76376	0.9747857	0.864379	6.772071
5	5.692656	72.50427	150.0229	2.82492816	27.29344942	0.998233	0.76376	0.9747857	0.805892	9.265758
6	6.626612	72.47452	136.0567	3.85119231	35.57737452	0.998233	0.76376	0.9747857	0.730869	12.07804
7	6.456571	72.37953	131.7711	4.64779314	43.27375564	0.998233	0.76376	0.9747857	0.707847	14.69086

			Liquid Carry-Over(LCO)[Oil/Water] [Slot (1)/Recombination (1)]			9-psig		Water cut	90%	
Runs	Pressure (Psig)	Temp (oF)	Rates Ql(lb/min)	Qg(lb/min)	Qg(ft3/min)	Water Density g/cc	Oil Density g/cc	Mix Density g/cc	Liq Vel (ft/sec)	Gas Vel (ft/sec)
0	9.921611	72.43332	305.4859	0	0	0.998233	0.76376	0.9747857	1.680479	0
1	9.794286	72.36466	298.3609	0.6452681	5.189032139	0.998233	0.76376	0.9747857	1.602733	1.761606
2	8.38662	72.36122	273.3759	1.05981236	9.042255323	0.998233	0.76376	0.9747857	1.468519	3.069724
3	8.447496	72.44247	257.6494	1.49628119	12.73455013	0.998233	0.76376	0.9747857	1.384039	4.323208
4	8.408137	72.44247	243.7599	2.14864721	18.31785381	0.998233	0.76376	0.9747857	1.309428	6.218665
5	8.257198	72.50198	241.2267	2.82085514	24.20944633	0.998233	0.76376	0.9747857	1.29582	8.218781
6	9.612563	72.46651	209.2152	3.97945728	32.24683695	0.998233	0.76376	0.9747857	1.123861	10.94737
7	9.366547	72.45163	197.7839	4.69399192	38.42469545	0.998233	0.76376	0.9747857	1.062454	13.04467

Table B.12 (continued)

Liquid Carry-Over(LCO)[Oil/Water] [Slot (1)/Recombination (1)]			3-psig				Water cut	70%		
Runs	Pressure (Psig)	Temp (oF)	Rates Ql(lb/min)	Qg(lb/min)	Qg(ft3/min)	Water Density g/cc	Oil Density g/cc	Mix Density g/cc	Liq Vel (ft/sec)	Gas Vel (ft/sec)
0	3.459391	72.45735	197.023	0	0	0.998233	0.76376	0.9278911	1.1386	0
1	3.414996	72.46651	142.8335	0.50286139	5.468951393	0.998233	0.76376	0.9278911	0.767272	1.856635
2	3.384151	72.38869	124.8786	0.8131102	8.856901595	0.998233	0.76376	0.9278911	0.670822	3.006799
3	2.896195	72.36694	118.7164	1.19129716	13.33564898	0.998233	0.76376	0.9278911	0.63772	4.527273
4	2.915632	72.36809	100.8866	1.63424058	18.2739108	0.998233	0.76376	0.9278911	0.541942	6.203747
5	2.900471	72.4482	89.55014	2.19706306	24.59219667	0.998233	0.76376	0.9278911	0.481045	8.348719
6	2.846856	72.45392	87.05361	3.12613149	35.09875244	0.998233	0.76376	0.9278911	0.467634	11.91555
7	3.31235	72.45049	70.95417	3.54618885	38.78577142	0.998233	0.76376	0.9278911	0.381151	13.16725

Liquid Carry-Over(LCO)[Oil/Water] [Slot (1)/Recombination (1)]			6-psig				Water cut	70%		
Runs	Pressure (Psig)	Temp (oF)	Rates Ql(lb/min)	Qg(lb/min)	Qg(ft3/min)	Water Density g/cc	Oil Density g/cc	Mix Density g/cc	Liq Vel (ft/sec)	Gas Vel (ft/sec)
0	6.824829	72.48768	240.5238	0	0	0.998233	0.76376	0.9278911	1.389992	0
1	6.737245	72.52144	186.4147	0.60393653	5.55087111	0.998233	0.76376	0.9278911	1.001381	1.884446
2	5.768406	72.51686	168.519	0.97735846	9.408165291	0.998233	0.76376	0.9278911	0.905249	3.193945
3	5.809733	72.47795	165.1736	1.43313049	13.76667578	0.998233	0.76376	0.9278911	0.887278	4.673601
4	5.782122	72.45392	149.6071	1.96762565	18.92567089	0.998233	0.76376	0.9278911	0.803659	6.42501
5	5.677791	72.39327	140.5982	2.64746099	25.59214801	0.998233	0.76376	0.9278911	0.755265	8.688189
6	6.609144	72.44591	133.1924	3.77011457	34.85505447	0.998233	0.76376	0.9278911	0.715482	11.83282
7	6.439391	72.50313	121.3508	4.28024994	39.89335271	0.998233	0.76376	0.9278911	0.651871	13.54326

Liquid Carry-Over(LCO)[Oil/Water] [Slot (1)/Recombination (1)]			9-psig				Water cut	70%		
Runs	Pressure (Psig)	Temp (oF)	Rates Ql(lb/min)	Qg(lb/min)	Qg(ft3/min)	Water Density g/cc	Oil Density g/cc	Mix Density g/cc	Liq Vel (ft/sec)	Gas Vel (ft/sec)
0	9.946537	72.49626	300.0142	0	0	0.998233	0.76376	0.9278911	1.733788	0
1	9.818892	72.48024	279.8084	0.6051444	4.862542397	0.998233	0.76376	0.9278911	1.503073	1.650768
2	8.407897	72.43218	253.1156	0.98126789	8.365524549	0.998233	0.76376	0.9278911	1.359684	2.839983
3	8.469137	72.48138	248.2559	1.44172927	12.25970461	0.998233	0.76376	0.9278911	1.333579	4.162005
4	8.429886	72.50427	225.0091	1.98336666	16.89485018	0.998233	0.76376	0.9278911	1.208702	5.735574
5	8.27876	72.51228	211.6003	2.6739356	22.92744751	0.998233	0.76376	0.9278911	1.136673	7.78356
6	9.637902	72.48367	200.5877	3.81535595	30.88587737	0.998233	0.76376	0.9278911	1.077516	10.48534
7	9.391469	72.47223	182.8756	4.34017344	35.49298125	0.998233	0.76376	0.9278911	0.98237	12.04939

Table B.12 (continued)

Liquid Carry-Over(LCO)[Oil/Water] [Slot (1)/Recombination (1)]						3-psig		Water cut	50%	
Runs	Pressure (Psig)	Temp (oF)	Rates Ql(lb/min)	Qg(lb/min)	Qg(ft3/min)	Water Density g/cc	Oil Density g/cc	Mix Density g/cc	Liq Vel (ft/sec)	Gas Vel (ft/sec)
0	3.459734	72.50141	189.2389	0	0	0.998233	0.76376	0.8809965	1.151827	0
1	3.415335	72.51228	136.7786	0.48154444	5.23746765	0.998233	0.76376	0.8809965	0.734746	1.77805
2	3.384823	72.53632	121.1816	0.78903785	8.596754656	0.998233	0.76376	0.8809965	0.650962	2.918482
3	2.897057	72.48253	110.3741	1.10758439	12.40063364	0.998233	0.76376	0.8809965	0.592907	4.209848
4	2.916789	72.51	98.08419	1.588845	17.76987056	0.998233	0.76376	0.8809965	0.526888	6.032632
5	2.90191	72.49054	84.6298	2.07634531	23.24092532	0.998233	0.76376	0.8809965	0.454614	7.889981
6	2.848551	72.41959	78.63079	2.92444559	32.82902912	0.998233	0.76376	0.8809965	0.422388	11.14501
7	3.31465	72.51343	66.10759	3.44982502	37.73145233	0.998233	0.76376	0.8809965	0.355116	12.80932

Liquid Carry-Over(LCO)[Oil/Water] [Slot (1)/Recombination (1)]						6-psig		Water cut	50%	
Runs	Pressure (Psig)	Temp (oF)	Rates Ql(lb/min)	Qg(lb/min)	Qg(ft3/min)	Water Density g/cc	Oil Density g/cc	Mix Density g/cc	Liq Vel (ft/sec)	Gas Vel (ft/sec)
0	6.842699	72.51171	236.1133	0	0	0.998233	0.76376	0.8809965	1.437135	0
1	6.754886	72.53975	178.5123	0.57833487	5.311374477	0.998233	0.76376	0.8809965	0.958931	1.80314
2	5.784229	72.52373	163.53	0.9484235	9.12269964	0.998233	0.76376	0.8809965	0.878449	3.097034
3	5.826393	72.49741	153.5668	1.33242402	12.78936658	0.998233	0.76376	0.8809965	0.824929	4.341818
4	5.799423	72.52716	145.4514	1.91296939	18.38695728	0.998233	0.76376	0.8809965	0.781335	6.242124
5	5.695488	72.48367	132.8731	2.5019961	24.16910404	0.998233	0.76376	0.8809965	0.713767	8.205085
6	6.630567	72.50771	124.5993	3.52688138	32.57737436	0.998233	0.76376	0.8809965	0.669322	11.05958
7	6.461066	72.46307	118.0532	4.1639388	38.76662625	0.998233	0.76376	0.8809965	0.634157	13.16075

Liquid Carry-Over(LCO)[Oil/Water] [Slot (1)/Recombination (1)]						9-psig		Water cut	50%	
Runs	Pressure (Psig)	Temp (oF)	Rates Ql(lb/min)	Qg(lb/min)	Qg(ft3/min)	Water Density g/cc	Oil Density g/cc	Mix Density g/cc	Liq Vel (ft/sec)	Gas Vel (ft/sec)
0	9.947525	72.48081	281.4551	0	0	0.998233	0.76376	0.8809965	1.713113	0
1	9.819866	72.52487	267.947	0.57949154	4.6566181	0.998233	0.76376	0.8809965	1.439356	1.580859
2	8.409566	72.53517	245.622	0.95221719	8.118845034	0.998233	0.76376	0.8809965	1.319431	2.756239
3	8.471659	72.49855	230.8109	1.34041856	11.39733905	0.998233	0.76376	0.8809965	1.239868	3.869243
4	8.433231	72.50771	218.7589	1.92827314	16.423279	0.998233	0.76376	0.8809965	1.175127	5.575482
5	8.282867	72.43675	199.9739	2.52701606	21.66075286	0.998233	0.76376	0.8809965	1.074219	7.353534
6	9.643639	72.407	187.6466	3.56920395	28.88227127	0.998233	0.76376	0.8809965	1.007999	9.805142
7	9.397991	72.49283	177.9062	4.22223394	34.52048894	0.998233	0.76376	0.8809965	0.955675	11.71924

Table B.12 (continued)

Liquid Carry-Over(LCO)[Oil/Water] [Slot (1)/Recombination (1)]						3-psig		Water cut	30%	
Runs	Pressure (Psig)	Temp (oF)	Rates Ql(lb/min)	Qg(lb/min)	Qg(ft3/min)	Water Density g/cc	Oil Density g/cc	Mix Density g/cc	Liq Vel (ft/sec)	Gas Vel (ft/sec)
0	3.593869	72.47166	176.883	0	0	0.998233	0.76376	0.8341019	1.137151	0
1	3.547749	72.43561	129.0159	0.45421501	4.90366751	0.998233	0.76376	0.8341019	0.693047	1.664729
2	3.237023	72.43904	115.7044	0.75337513	8.274324197	0.998233	0.76376	0.8341019	0.62154	2.809022
3	2.962135	72.45049	105.7538	1.06122039	11.83704588	0.998233	0.76376	0.8341019	0.568088	4.018518
4	2.997005	72.40356	96.40275	1.56160766	17.3826038	0.998233	0.76376	0.8341019	0.517856	5.90116
5	2.99163	72.50771	79.70946	1.95562756	21.77940068	0.998233	0.76376	0.8341019	0.428183	7.393813
6	2.955507	72.50313	70.55205	2.84713266	31.77250065	0.998233	0.76376	0.8341019	0.378991	10.78634
7	3.281065	72.50656	63.81783	3.33033387	36.492117	0.998233	0.76376	0.8341019	0.342816	12.38858

Liquid Carry-Over(LCO)[Oil/Water] [Slot (1)/Recombination (1)]						6-psig		Water cut	30%	
Runs	Pressure (Psig)	Temp (oF)	Rates Ql(lb/min)	Qg(lb/min)	Qg(ft3/min)	Water Density g/cc	Oil Density g/cc	Mix Density g/cc	Liq Vel (ft/sec)	Gas Vel (ft/sec)
0	6.468974	72.53117	193.2319	0	0	0.998233	0.76376	0.8341019	1.242255	0
1	6.385956	72.52373	168.3811	0.54551223	5.097437148	0.998233	0.76376	0.8341019	0.904508	1.730511
2	5.9091	72.53288	156.1388	0.9055569	8.657746754	0.998233	0.76376	0.8341019	0.838745	2.939188
3	5.936067	72.53174	147.1384	1.27664813	12.18965773	0.998233	0.76376	0.8341019	0.790397	4.138225
4	5.928667	72.53059	142.9579	1.88017562	17.95864425	0.998233	0.76376	0.8341019	0.76794	6.096718
5	5.883022	72.53861	125.1479	2.35653121	22.55884632	0.998233	0.76376	0.8341019	0.672268	7.658424
6	6.353866	72.52602	121.3053	3.43364198	32.13406826	0.998233	0.76376	0.8341019	0.651627	10.90908
7	6.314932	72.52487	113.9642	4.01971299	37.68848469	0.998233	0.76376	0.8341019	0.612192	12.79473

Liquid Carry-Over(LCO)[Oil/Water] [Slot (1)/Recombination (1)]						9-psig		Water cut	30%	
Runs	Pressure (Psig)	Temp (oF)	Rates Ql(lb/min)	Qg(lb/min)	Qg(ft3/min)	Water Density g/cc	Oil Density g/cc	Mix Density g/cc	Liq Vel (ft/sec)	Gas Vel (ft/sec)
0	9.934568	74.94688	247.9965	0	0	0.998233	0.76376	0.8341019	1.594328	0
1	9.807076	74.62944	242.74	0.54660326	4.411998059	0.998233	0.76376	0.8341019	1.303949	1.497814
2	8.398093	74.78765	234.5204	0.90917913	7.78854677	0.998233	0.76376	0.8341019	1.259795	2.644107
3	8.459577	74.9462	221.1491	1.28430802	10.9761592	0.998233	0.76376	0.8341019	1.187967	3.726258
4	8.420684	75.10509	191.0087	1.89521703	16.22927316	0.998233	0.76376	0.8341019	1.026059	5.50962
5	8.270033	75.26431	188.3476	2.38009652	20.52121037	0.998233	0.76376	0.8341019	1.011764	6.966674
6	9.628101	75.42387	182.6858	3.47484569	28.29611206	0.998233	0.76376	0.8341019	0.98135	9.606149
7	9.382269	74.40971	175.744	4.07598897	33.46660516	0.998233	0.76376	0.8341019	0.944061	11.36146

Table B.12 (continued)

Liquid Carry-Over(LCO)[Oil/Water] [Slot (1)/Recombination (1)]			3-psig				Water cut	10%		
Runs	Pressure (Psig)	Temp (oF)	Rates Ql(lb/min)	Qg(lb/min)	Qg(ft3/min)	Water Density g/cc	Oil Density g/cc	Mix Density g/cc	Liq Vel (ft/sec)	Gas Vel (ft/sec)
0	3.65643	72.47166	185.3021	0	0	0.998233	0.76376	0.7872073	1.262241	0
1	3.609507	72.43561	139.7007	0.42141971	4.534266183	0.998233	0.76376	0.7872073	0.750443	1.539322
2	3.158505	72.43904	128.0655	0.67759183	7.474715712	0.998233	0.76376	0.7872073	0.687941	2.537565
3	2.990543	72.45049	98.82334	0.99167439	11.04355463	0.998233	0.76376	0.7872073	0.530859	3.749138
4	3.032774	72.40356	86.08989	1.39455196	15.49175817	0.998233	0.76376	0.7872073	0.462457	5.259243
5	3.031993	72.50771	55.8716	1.86146772	20.68357319	0.998233	0.76376	0.7872073	0.300131	7.021794
6	3.004395	72.50313	49.70912	2.52107378	28.05616717	0.998233	0.76376	0.7872073	0.267027	9.524691
7	3.258727	72.50656	30.24407	3.07978792	33.78873665	0.998233	0.76376	0.7872073	0.162465	11.47082

Liquid Carry-Over(LCO)[Oil/Water] [Slot (1)/Recombination (1)]			6-psig				Water cut	10%		
Runs	Pressure (Psig)	Temp (oF)	Rates Ql(lb/min)	Qg(lb/min)	Qg(ft3/min)	Water Density g/cc	Oil Density g/cc	Mix Density g/cc	Liq Vel (ft/sec)	Gas Vel (ft/sec)
0	3.424711	72.43618	205.3332	0	0	0.998233	0.76376	0.7872073	1.100892	0
1	6.720276	72.52373	176.2236	0.50612507	4.655576451	0.998233	0.76376	0.7872073	0.946637	1.580505
2	5.753734	72.53288	160.4325	0.81446538	7.845997745	0.998233	0.76376	0.7872073	0.86181	2.663611
3	5.794811	72.53174	127.4959	1.1929843	11.46932938	0.998233	0.76376	0.7872073	0.684881	3.893683
4	5.767127	72.53059	107.6648	1.67904056	16.16406487	0.998233	0.76376	0.7872073	0.578353	5.487482
5	5.662926	72.53861	87.12224	2.2430686	21.70477023	0.998233	0.76376	0.7872073	0.468003	7.368477
6	6.591676	72.52602	72.41322	3.04041498	28.13620832	0.998233	0.76376	0.7872073	0.388989	9.551864
7	6.422212	72.52487	65.3905	3.71730402	34.67610466	0.998233	0.76376	0.7872073	0.351264	11.77207

Liquid Carry-Over(LCO)[Oil/Water] [Slot (1)/Recombination (1)]			9-psig				Water cut	10%		
Runs	Pressure (Psig)	Temp (oF)	Rates Ql(lb/min)	Qg(lb/min)	Qg(ft3/min)	Water Density g/cc	Oil Density g/cc	Mix Density g/cc	Liq Vel (ft/sec)	Gas Vel (ft/sec)
0	9.941046	74.94688	244.4002	0	0	0.998233	0.76376	0.7872073	1.664806	0
1	9.813471	74.62944	234.4916	0.50713732	4.092374324	0.998233	0.76376	0.7872073	1.25964	1.389306
2	8.403829	74.78765	200.9296	0.81772324	7.003344165	0.998233	0.76376	0.7872073	1.079352	2.377541
3	8.465618	74.9462	176.6563	1.2001422	10.25417328	0.998233	0.76376	0.7872073	0.948961	3.481154
4	8.426958	75.10509	122.0078	1.69247288	14.48918692	0.998233	0.76376	0.7872073	0.655401	4.918884
5	8.27645	75.26431	97.27897	2.26549928	19.52769655	0.998233	0.76376	0.7872073	0.522562	6.62939
6	9.63587	75.42387	89.7643	3.07689996	25.0475904	0.998233	0.76376	0.7872073	0.482195	8.503319
7	9.39013	74.40971	78.82348	3.76934628	30.9387638	0.998233	0.76376	0.7872073	0.423423	10.50329

VITA

Adedeji Adebare completed both his Bachelor of Science and Master of Science degrees in Nigeria from Obafemi Awolowo University Ile-Ife in December 1996 and University of Lagos, Lagos in January 2001 respectively. My email address is dejiadebare@yahoo.com.